Cell surface localisation of GPI-anchored receptors in *Trypanosoma brucei*

Sourav Banerjee[1*], Nicola Minshall[1*], Alex Cook[2,3], Olivia Macleod[1], Helena Webb[1], Matthew Higgins[2,3] and Mark Carrington[1]

[1] Department of Biochemistry, University of Cambridge, Tennis Court Road, Cambridge CB2 1QW, UK.

[2] Department of Biochemistry, University of Oxford, South Parks Road, Oxford OX1 3QU, UK.

[3]Kavli Institute for Nanoscience Discovery, Dorothy Crowfoot Hodgkin Building, University of Oxford, South Parks Rd, Oxford, OX1 3QU, UK.

* These authors made equal contributions

Correspondence: Mark Carrington: mc115@cam.ac.uk

ABSTRACT

Trypanosoma brucei, the causal agent of Human and Animal African trypanosomiasis proliferates in the extracellular milieu of mammals. It acquires host macromolecular nutrients, by receptor mediated endocytosis. The best characterised receptor is for transferrin (TfR) and it has been reported to be sequestered in the flagellar pocket, the sole site of endocytosis. In this location the TfR may be inaccessible to adaptive immune system effectors. The *T. brucei* genome encodes ~15 TfR variants, and here we compared two, the first attached to the plasma membrane by a single glycosylphosphoinositol (GPI)-anchor and the other by two. Transferrin uptake kinetics were similar and rapid for both. Unexpectedly, initial binding of transferrin occurred over the whole cell surface suggesting the TfR was not sequestered in the flagellar pocket. This localisation was confirmed by immunofluorescence assays and was independent of the number of GPI-anchors. Two other GPI-anchored receptors were investigated to determine whether localisation to the whole cell surface was a general property of GPI-anchored receptors. Haptoglobin-haemoglobin uptake assays and immunofluorescence localisation of complement factor H receptor showed both were also whole cell surface localised. The mechanisms by which trypanosome receptors are protected from antibody-mediated attack are more subtle than hiding in a pocket.

INTRODUCTION

Trypanosoma brucei proliferates within the bloodstream and tissue spaces of mammals and can maintain a long-term infection lasting in some cases for years. To do this, it must avoid the host adaptive and innate immune response at the same time as acquiring nutrients from the host. The adaptive immune response is overcome through a population survival strategy based on a densely packed surface coat of variant surface glycoprotein (VSG) that undergoes antigenic variation. As the antibody titre against one VSG increases, a small subset of trypanosomes that have switched expression to a different VSG escape until they are recognised in turn and so on in an iterative process (Mugnier et al., 2015). The trypanosome has evolved mechanisms to increase the titre of host immunoglobin required for killing. First, there is rapid endocytosis and degradation of VSG bound antibody (Engstler et al., 2007) and second, a receptor for IgG Fc region (ISG75) inhibits the classical pathway of complement and C1q and Fc-dependent phagocytosis (Mikkelsen et al., 2024). How the innate immune system is countered is less well understood (Pinger et al., 2018) but receptors for Complement C3 (C3R also known as ISG65) and Factor H (FHR) have been identified and characterised (Cook et al., 2024; Macleod et al., 2020, 2022). Acquisition of small molecule nutrients, such as glucose and amino acids, use typical eukaryotic membrane transporters.

Obtaining host macromolecule nutrients poses a more complex problem. First, *T. brucei* has a very wide host range and receptors have to recognise a diversity of ligands, this has been shown to be the case for both the transferrin (TfR) (Trevor et al., 2019) and haptoglobin haemoglobin receptors (HpHbR) (Lane-Serff et al., 2016). Second, as these receptors bind ligands that are equivalent in size to immunoglobulin molecules then why are host antibodies against receptors not sufficient to clear an infection? Some models to account for this suggested that the VSG coat acts as a barrier preventing immunoglobulin access. However, it was shown that antibodies could penetrate a significant distance into the VSG coat (Hsia et al., 1996) but not to the small plasma membrane proximal VSG domain (Schwede et al., 2011). Both the ligand size and the penetration of antibodies into the VSG coat made it unlikely that receptors were sterically protected from antibody binding. Immunization of mice with neither recombinant C3R nor ISG75 protected against infection (Ziegelbauer & Overath, 1993). In addition, accessibility of the HpHbR was demonstrated by the ability of a monoclonal antibody drug conjugate to clear infections in a mouse model (MacGregor et al., 2019).

The trypanosome flagellar pocket is an invagination of the plasma membrane at the base of the single flagellum and is the sole site of endo- and exocytosis. The flagellar pocket is a discrete domain of the plasma membrane (Gadelha et al., 2009) with several exclusively localised proteins (Gadelha et al., 2015). At the neck of the pocket, there is a restriction introduced by close contact between the plasma membranes of the flagellum and pocket as it emerges onto the cell body. This flagellar pocket collar is maintained by specific proteins (Bonhivers et al., 2008) and contains a specialised region of plasma membrane (Gadelha et al., 2009). The exclusive localisation of some proteins to the plasma membrane of the flagellar pocket, others to the cell body, and a range to both, indicates that there is regulated passage between the two domains of the plasma membrane.

There is variation in the reported localisation of receptors to different domains of the plasma membrane. TfR was the first receptor to be identified, it is glycosylphosphatidylinositol (GPI)-anchored and has been localised to the flagellar pocket and endosomal membrane in some studies but others suggested it was on the flagellar pocket, cell body plasma membrane and endosomal membrane (Duncan et al., 2024; Mussmann et al., 2003, 2004; Steverding et al., 1994a, 1995; Tiengwe et al., 2017). The Complement Factor H receptor (FHR) is probably GPI-anchored and is localised to the cell body and flagellar plasma membrane (Macleod et al., 2020). HpHbR, also probably GPI-anchored, has been localised to the flagellar pocket (Vanhollebeke et al., 2008). C3R and ISG75 are type I transmembrane proteins and localise to the cell body, flagellar and pocket plasma membrane (Leung et al., 2011; Ziegelbauer et al., 1992). The localisation of receptors to the flagellar pocket has been proposed to protect the cell from downstream effects of antibody recognition of the receptor but the discovery of new receptors, such as C3R (Macleod et al., 2022) and FHR (Macleod et al., 2020) that are more abundant and distributed over the cell surface seems to contradict this argument.

Newly synthesised or recycled proteins are added to the plasma membrane at the flagellar pocket. For proteins that are concentrated in the flagellar pocket, the nature of the retention and/or retrieval signal is unknown but for transmembrane proteins could involve recognition in the cytoplasm. In contrast, GPI-anchored proteins have no cytoplasmic component and recognition must occur on the external face of the plasma membrane. Any signal for retention has to operate in a background of huge sequence variation in VSGs which makes short amino acid motifs unlikely. There is experimental evidence that one such signal is the number of GPI-anchors per molecule, a single anchor leading to retention and more than one escape to the surface of the cell body (Tiengwe et al., 2017). These experiments manipulated the number of GPI-anchors on TfR, usually a heterodimer with a single anchor on one subunit. Adding an anchor to the second subunit caused a change in localisation to

128 the cell surface and endosome as judged by immunofluorescence. However, conditions that
129 led to in a few fold increase in expression of single GPI- anchored TfR, including transferrin
130 shortage and growth at high cell density, resulted in the detection of TfR on the cell body
131 surface (Mussmann et al., 2004). Whether the surface-localized TfR is functional remains
132 unproven (Mussmann et al., 2004; Schwartz et al., 2005).
133
134 TfR is encoded by a dispersed gene family with ~15 TfR variants. The experiments here
135 started with a chance observation that one of these encoded a receptor with two GPI-
136 anchors while the others have a single anchor. This was exploited to investigate how the
137 presence of one or two GPI-anchors affected function. We show that the second GPI-anchor
138 has no effect on the kinetics of uptake, or processing of transferrin through the endosome.
139 However, the second anchor resulted in ≥1.5-fold increase in steady state receptor levels.
140 Further, transferrin uptake experiments provided evidence that TfR was present over the
141 entire cell surface and this was supported by immunofluorescence experiments. An analysis
142 of the localisation of two other putatively GPI-anchored proteins showed that all were
143 present over the entire cell surface. These experiments demonstrate that the trypanosome
144 expresses a set of receptors over the entire cell surface inferring that there are robust
145 mechanisms to resist antibody mediated recognition of conserved cell surface proteins.
146
147 **RESULTS**
148
149 **The BES7 VSG expression site encodes a transferrin receptor with two GPI-anchors**
150
151 In *T. brucei*, the active VSG gene is transcribed from a bloodstream form expression site
152 (BES) that is telomere proximal. BESs contain up to 12 other co-transcribed expression site
153 associated genes (ESAGs) (Hertz-Fowler et al., 2008; Pays et al., 2001). TfRs are
154 heterodimers encoded by ESAG6 and ESAG7 (Chaudhri et al., 1994; Salmon et al., 1994a)
155 and those characterised to date are attached to the external face of the plasma membrane
156 by the addition of a GPI-anchor to ESAG6. The ESAG6 and 7 subunits share around 80%
157 amino acid identity and different BESs encode variants of ESAG6 and 7 with 90% or more
158 amino acid sequence identity (Maier & Steverding, 2008; Trevor et al., 2019). In *T. brucei*
159 Lister 427, the isolate used in these experiments, there are 15 BESs (Barcons-Simon et al.,
160 2023) and most were sequenced and annotated after transformation associated
161 recombination cloning of telomeres (Hertz-Fowler et al., 2008). In the original annotation,
162 BES7 stands out as it has two copies of ESAG6 but apparently lacked ESAG7 and as such
163 would not be able to make a functional TfR. Here, a fresh analysis of the sequence was
164 performed and indicated that the first 'ESAG6' gene annotated in BES7 actually encoded an

ESAG7 with a GPI-anchor. Phylogenetic analysis of ESAG6 and ESAG7 confirmed that a copy of ESAG7 is indeed present in BES7 along with a single copy of ESAG6 (Figure 1A). The origin of the GPI-anchor attachment signal in BES7 ESAG7 was investigated by comparing the ESAG7 mRNA sequences from 13 different BESs. This showed that all the ESAG7 genes contained residual coding sequences for GPI-anchor addition but a set of small deletions between nucleotides 985 and 1068 in the ORF resulted in a frameshift leading to a premature stop codon at the C-terminal end effectively removing the GPI-anchor attachment sequence (Figure S1). A comparison of BES7 ESAG6 and 7 showed that the C-terminal 120 amino acid sequences are identical and there was a clear prediction for a GPI-anchor on both using NetGPI 1.1 (Gíslason et al., 2021) (Figure S2).

Cellular TfR protein levels are determined by BES identity and the number of GPI-anchors

ESAG6 and 7 protein levels were examined by western blotting in cell lines expressing VSGs and TfRs from three different BESs: BES3-VSG118, BES1-VSG221 and BES7-VSG224 (Figure 1B). TfRs have several N-linked glycosylation sites and whole cell lysates were treated with PNGaseF to simplify analysis. First, in BES7 cells there was a shift in the apparent molecular weight of ESAG7 from ~30 kDa to ~38 kDa, which is consistent with the addition of a GPI-anchor (Figure 1B), such a change in mobility on the addition of a GPI-anchor to ESAG7 has been reported previously (Tiengwe et al., 2017). Second, the identity of the active BES affected both ESAG6 and ESAG7 protein levels, there were increasing levels of expression: BES3 < BES1 < BES7 (Figure 1B). Lastly, when the BES7 cell line was modified to exchange VSG224 to VSG221 (see below), this had little effect on TfR expression, suggesting the BES identity was the dominant determinant rather than the VSG type. The rabbit TfR antiserum used was raised against the TfR from BES1 (Gerrits et al., 2002) and is the same as used in most other studies (Mussmann et al., 2003; Tiengwe et al., 2017). The amino acid sequence identity between BES2 TfR and BES1 TfR is >98% and BES7 TfR is >92% and it is unlikely that the difference in TfR levels result from differential reactivity of the serum to different TfRs.

We next investigated whether GPI-anchor number contributed to the variation in cellular TfR levels by making a set of transgenic cell lines (Figure 2A). First, VSG224 in BES7 was changed to VSG221. Next, the cell line expressing VSG221 from BES7 was modified to alter the ESAG7 by exchanging the 3' end of the ORF with that from BES1 ESAG7 resulting in the loss of the GPI-anchor signal. As a control, a second cell line in which the ESAG7 gene retained the GPI-anchor addition sequence was made. Similar modifications were performed

201 on cells expressing VSG221 from BES1, cell lines expressing either BES1 ESAG7 modified
202 with the C-terminal GPI-anchor sequence from BES7 ESAG7 or the endogenous BES1
203 ESAG7 were made. The result was four cell lines: all expressed VSG221 from either BES1
204 or BES7 and TfR with or without a GPI-anchor on ESAG7.
205
206 The cell lines were characterised by western blotting of PNGaseF-treated whole cell lysates
207 (Figure 2B). The addition of a GPI-anchor signal sequence to ESAG7 resulted in an increase
208 in both ESAG6 and 7. To estimate this change, whole cell lysates were minimally separated
209 by SDS-PAGE to collapse the ESAG6 and 7 proteins into a single band prior to western
210 blotting. Relative quantitation was obtained using a titration curve of the highest TfR
211 expresser and normalised against SCD6 for loading (Figure 2C). Three biological replicates
212 were performed and the levels of both TfRs from BES1 is significantly lower ($p>0.99$), ~3.5
213 fold, compared to BES7, regardless of GPI-anchor number. The presence of a GPI-anchor
214 on ESAG7, leading to a double-anchored TfR, significantly increased ($p>0.95$) the
215 expression level by approximately 1.9-fold in BES1 and about 1.5-fold in BES7. This
216 provides strong evidence that the presence of a GPI-anchor on ESAG7 contributes to the
217 higher cellular expression level of TfR, which could result from increased protein stability,
218 reported for VSGs, (Bangs et al., 1986; Engstler et al., 2004) or a higher rate of turnover
219 and/or greater shedding of the single GPI-anchored TfR.
220
221 **Transferrin uptake kinetics are similar in cells expressing TfRs with either one or two**
222 **GPI-anchors**
223
224 To investigate whether anchor number influenced function, BES7-VSG221 cell lines
225 expressing single or double GPI-anchored TfR were used. It has already been shown that a
226 TfR with double GPI-anchors is functional (Tiengwe et al., 2017), here the kinetics of
227 transferrin binding and uptake by single and double GPI-anchor TfRs were compared. The
228 experimental approach was similar to that developed to characterise the binding and
229 endocytosis of VSG antibodies (Engstler et al., 2007). The medium used to culture
230 trypanosomes contained ~2.5 μM transferrin (Kakuta et al., 1997), Alexa 568 labelled bovine
231 holo-transferrin (Tf_{A568}) was added to cultures, without any other manipulation, to a final
232 concentration of 0.5 μM and cells were then fixed over a time course from 15 to 600 seconds
233 and imaged by epifluorescence microscopy (Figure 3A and S3A). At 15 seconds there was
234 variation between individual cells with Tf_{A568} present on the flagellum, across the cell body
235 and the flagellar pocket in both cell lines. There was also variation at 60 seconds, Tf_{A568} was
236 present in the endosomal compartment of most cells, and the cell surface in some cells. At

600 seconds the Tf_{A568} was predominantly within the endosomal compartment. The variation was also examined by quantifying the fluorescence from individual cells (Figure 3B), this showed the range of variation and an increase in fluorescence between 15 and 60 seconds followed by a decrease by 600 seconds. Fluorescence intensity was also determined across transverse sections of the cell (Figure 3C), this showed some cells with internal signal and others with two peaks from a cell surface distribution. There was a stronger signal from cells expressing TfR with two GPI-anchors, consistent with higher expression levels, but no consistent differences in distribution were seen.

The same Tf_{A568} uptake assay was performed with the BES1-VSG221 cells expressing TfRs with one or two GPI-anchors (Figure 3D and S3B). There was a reduced binding and uptake of Tf_{A568} in BES1 cells compared to BES7 cells as might be expected given lower levels of the receptor. Otherwise, the time course of uptake was similar: at 15 seconds Tf_{A568} was present on the flagellum and cell body surface as well as the flagellar pocket in both cell lines, at 60 seconds Tf_{A568} on the cell surface was reduced and some was now present in the flagellar pocket and endosomal compartments, and by 600 seconds Tf_{A568} was substantially within endosomal compartments. In both BES7 and BES1 cell lines, fluorescence distribution patterns across the cells showed variability at 15 and 60 sec (Figure 3E-F), but appeared more uniform at 600 sec.

Previous studies have shown that some TfRs do not bind canine transferrin (Mussmann et al., 2003). Canine transferrin has 501/686 amino acid sequence identities with bovine transferrin (Figure S4A) and it was used as a negative control in the same transferrin binding and uptake assay above using BES7-VSG221 cells expressing TfR with either one or two GPI-anchors (Figure S4B). No cell binding or uptake of canine Tf in either cell line was observed. These findings provide evidence that the binding of bovine transferrin to the cell surface is receptor dependent. Together, these experiments support a model in which the TfR is present on the cell surface, and endocytosis is a rapid process. The greater Tf binding and uptake in BES7 compared to BES1 cells provides evidence that TfR abundance limits the amount of Tf endocytosed. The number of GPI-anchors on the TfR has no obvious influence on Tf uptake but does affect receptor levels.

The finding that Tf_{A568} was bound over the whole cell surface at early time points in the uptake assays suggested a similar localisation for the TfR. This is not consistent with some previous studies that found TfR and other GPI-anchored receptors sequestered in the flagellar pocket (Duncan et al., 2024; Mussmann et al., 2004; Steverding et al., 1994a, 1995; Tiengwe et al., 2017; Vanhollebeke et al., 2008) or that expression level determined

274 localisation (Mussmann et al., 2003). We went on to characterise the cellular localisation of
275 single and double GPI-anchored TfR along with two other GPI-anchored receptors.
276
277 **Localisation of the transferrin receptor by immunofluorescence**
278
279 Previous reports provided evidence that in BES1-VSG221 cells grown in the presence of
280 10% FBS, the cell surface TfR is located within the flagellar pocket, rather than dispersed on
281 the cell surface (Ligtenberg et al., 1994; Mussmann et al., 2003; Salmon et al., 1994a;
282 Tiengwe et al., 2017). In contrast, when cells are treated to increase TfR expression by
283 roughly three to fivefold, for example when grown to high density or in canine serum, TfR
284 localizes on the cell surface (Mussmann et al., 2003). The transferrin uptake experiments
285 above indicated that the TfR is dispersed over the cell surface and to resolve this
286 discrepancy, the localisation of the TfR was investigated using immunofluorescence. Based
287 on the transferrin uptake experiments, we reasoned that the localisation of the TfR would be
288 very dynamic and thus chose to fix the cells in culture without any centrifugation or washing.
289
290 Four cell lines, BES1-VSG221 and BES7-VSG221 cells each expressing TfR with one or two
291 GPI-anchors, were investigated. Fixative was added to cells in culture without any other
292 manipulations, the final concentrations were 4% formaldehyde and 0.2% glutaraldehyde and
293 TfR localisation was observed by immunofluorescence after settling cells on microscope
294 slides. Under these experimental conditions, the TfR in all four cell lines had a distribution
295 across the entire cell surface including the flagellar pocket and in internal compartments in
296 some cells (Figure 4A). Fluorescence intensity measurements across transverse sections of
297 both the BES7 1- and 2 GPI cells confirmed that TfR is indeed present on the surface of
298 some cells as seen by two peaks in fluorescence corresponding to the cell periphery in some
299 cells (Figure 4B). As in the Tf uptake experiments, the strength of signal as measured by
300 total fluorescence intensity from individual cells showed that TfR abundance varied between
301 individual cells in populations (Figure 4C and Figure S5). These measurements also showed
302 that the presence of two GPI-anchors on TfR increased levels by about 1.5-fold compared to
303 the single anchored receptor and that there is a ~3.5-fold higher TfR expression in BES7
304 compared to BES1 cells regardless of GPI-anchor number. These measurements support
305 the western blot quantitation (Figure 2) and also provide evidence that the
306 immunofluorescence signal does not contain a significant level of non-specific background.
307
308 Structured Illumination Microscopy (SIM) was used to obtain more information on TfR
309 localisation in the same four cell lines as above (Figure 5). TfR was present on the cell
310 surface including the flagellar pocket, cell body and flagellum, and in the endosome (single

311 stack images) (Figure 5A). Three-dimensional reconstruction of the localization of TfR
312 confirmed that it is distributed across the cell surface and in endosomes (Figure 5B).
313
314 These experiments collectively provide strong evidence that TfR is indeed present on the *T.*
315 *brucei* cell surface under normal growth conditions and that the localization pattern is
316 independent of the presence or absence of a GPI-anchor in the ESAG7 subunit.
317
318 **Cell surface localisation is shared by two other GPI-anchored receptors**
319
320 The finding that TfR is distributed over the whole cell surface led to an investigation of other
321 receptors. Two were selected on the basis of being predicted to have one or more GPI-
322 anchors and a non-expressing negative control being available. The first was the
323 haptoglobin haemoglobin receptor (HpHbR) for which +/+ and -/- cell lines were used. The
324 structure of most of HpHbR is known and it would appear to be a monomer but two or more
325 receptors can bind a single ligand (Higgins et al., 2013; Lane-Serff et al., 2014). HpHbR has
326 a low copy number, 300 to 400 per cell (Vanhollebeke et al., 2008) and, in the absence of a
327 suitable antibody, a ligand uptake assay was used. The second receptor analysed was the
328 complement factor H receptor (FHR), this was used after a fortuitous observation that
329 although it is not expressed when cells are grown in medium containing 10% foetal bovine
330 serum (Macleod et al., 2020), it is expressed at high levels when the same cells are grown in
331 medium with 10% rabbit serum replacing the foetal bovine serum. The structure of FHR is
332 known and it is a monomer with a single GPI-anchor (Macleod et al., 2020).
333
334 Alexa 568-labelled HpHb ($HpHb_{A568}$) was used in uptake assays with HpHbR +/+ and -/-
335 cells as for transferrin uptake (Figure 6A). There was binding of ligand to the cell surface by
336 15 seconds, uptake into the endosome by 60 seconds, and a location consistent with the
337 lysosome by 600 seconds. Binding and uptake were not detected in HpHbR -/- cells (Figure
338 6A). The kinetics of uptake were similar to those for transferrin. Presence of $HpHb_{A568}$ on the
339 cell surface was confirmed by the fluorescence signal measurement across the cells at 15
340 seconds, which showed two distinct peaks consistent with peripheral localisation for some
341 cells (Figure 6B), the noise in the quantification is due to the low copy number of the
342 receptor. Again, there was variability in binding and uptake of HpHb across the population
343 (Figure S6).
344
345 In trypanosomes cultured in medium containing 10% rabbit serum, expression of the FHR
346 was readily detected whereas in medium containing foetal bovine serum (FBS) it is not
347 (Figure 7A). Cells cultured with rabbit serum were used to determine the localisation of FHR

348 by immunofluorescence following the same procedure used for the transferrin receptor
349 (Figure 7B). The FHR was clearly localised over the entire cell surface. Two controls for
350 specificity of antibody binding were performed: first cells were grown in medium
351 supplemented with foetal bovine serum and second with a no primary antibody control for
352 the cells grown with rabbit serum to control for cell surface immunoglobulin originating from
353 the growth medium. Neither control gave a signal (Figure S7). SIM analysis further provided
354 spatial resolution along with reconfirming the distribution of the FHR across the trypanosome
355 cell surface and flagellum as well as within the flagellar pocket (Figure 7C).
356
357 These experiments show that the detection of TfR on the cell surface is part of a general
358 pattern where GPI-anchored receptors are distributed across the cell body plasma
359 membrane.
360
361 **DISCUSSION**
362
363 Any pathogen that has evolved to establish and maintain a long-term infection within a
364 mammalian host must be able to acquire nutrients as well as be resistant to both the innate
365 and adaptive immune responses of the host. African trypanosomes have evolved a strategy
366 that is dependent on variant surface glycoprotein (VSG), a superabundant protein that forms
367 a densely packed coat on the cell surface. Low frequency switching to a different VSG
368 allows the population to persist (Mugnier et al., 2015). The VSG coat appears to prevent
369 antibodies, and possibly innate immunity factors, gaining immediate access to the plasma
370 membrane (Schwede et al., 2011). However, such a coat cannot be totally impermeable as
371 trypanosomes require host macromolecules such as transferrin and haptoglobin-
372 haemoglobin which they acquire through receptor mediated endocytosis (Lane-Serff et al.,
373 2014; Salmon et al., 1994b; Steverding et al., 1994b, 1995; Trevor et al., 2019; Vanhollebeke
374 et al., 2008).
375
376 Why these receptors do not result in the trypanosomes becoming susceptible to immune
377 recognition and attack is central to understanding the mechanisms of infection (Banerjee et
378 al., 2024). One model proposed that the receptors are sequestered in the flagellar pocket, an
379 invagination of the plasma membrane at the base of the flagellum, and are not accessible to
380 immune effectors. The idea that sequestration in the flagellar pocket allowed receptors to
381 hide from host immune effectors was first challenged by the discovery of invariant surface
382 glycoproteins (ISGs) (Ziegelbauer et al., 1992; Ziegelbauer & Overath, 1992) that were
383 shown to be distributed over the whole cell surface (Macleod et al., 2022; Ziegelbauer &
384 Overath, 1993). Two ISGs were subsequently identified as receptors, one for complement

385 C3 and another for the Fc region of immunoglobulins (Macleod et al., 2022; Mikkelsen et al.,
386 2024). Both the ability to access ligands and the structures of the extracellular domains of
387 both ISGs indicated that they were unlikely to be physically shielded by the VSG coat. The
388 ISGs are type 1 transmembrane proteins with a large extracellular domain, a single
389 transmembrane pass and a small cytoplasmic tail. In contrast, VSGs have two or more GPI-
390 anchors whereas the two characterised nutrient receptors have a single GPI-anchor. Could
391 this difference in GPI-anchor number result in selective retention of nutrient receptors in the
392 flagellar pocket (Tiengwe et al., 2017) as it is difficult to envisage a requirement for any
393 amino acid sequence motifs in the context of variation of VSGs.
394
395
396 Here, we have investigated the distribution of GPI-anchored receptors on the cell surface of
397 mammalian infective *Trypanosoma brucei*. The main findings are: (1) The majority of TfRs
398 encoded in the genome have a single GPI-anchor but there is at least one with two GPI-
399 anchors. (2) The single anchored TfRs probably arose from loss of one anchor as opposed
400 to gain in the double anchored version. The loss of the GPI-anchor from ESAG7 may
401 provide a selective advantage possibly reducing exposure to the host adaptive immune
402 system without affecting transferrin acquisition (Trevor et al., 2019). (3) The steady state
403 level of TfR varies with the identity of the transcribed BES. (4) Single or double anchored
404 TfRs bind transferrin, as previously reported (Tiengwe et al., 2017) and result in similar
405 kinetics of transferrin uptake, with movement from the cell surface to the endosome
406 occurring within two minutes. The rapid kinetics of uptake indicates the receptor ligand
407 complex is probably subject to the same hydrodynamic forces as antibody VSG complexes
408 (Engstler et al., 2007) resulting in a directional movement towards the posterior end of the
409 cell, the location of the flagellar pocket and endocytosis. (5) Adding a second GPI-anchor to
410 a TfR resulted in a ~1.5-fold increase in cellular receptor levels. (6) Both single and double
411 GPI-anchored TfRs are present over the whole cell surface as seen by both transferrin and
412 antibody binding. (7) Two other GPI-anchored receptors, the HpHbR and FHR, both
413 probably with a single GPI-anchor, are present over the whole cell surface.
414
415 The earlier findings that the TfR, and subsequently the HpHbR, are localised to the flagellar
416 pocket is an attractive model as it provided an easy explanation for why the receptors did not
417 result in immune attack. The experiments presented here do not agree with this model and it
418 is worth discussing the reasons why these experimental differences have arisen. Here the
419 cells were fixed in culture using formaldehyde and a higher concentration (0.2%) of
420 glutaraldehyde than in previous reports. In contrast, much of the previous work involved
421 manipulations of the trypanosomes before determining either transferrin binding or TfR/

422 HpHbR localisation by immunofluorescence. The most common is centrifugation and
423 washing prior to fixation for immunofluorescence (Engstler et al., 2004; Roggy & Bangs,
424 1999; Tiengwe et al., 2017; Vanhollebeke et al., 2008), a process that is slow when
425 compared to the very rapid endocytosis of surface bound transferrin (Figure 3) and providing
426 time for the ligand bound receptors to be cleared from the cell surface. This would be even
427 more apparent if the experimental manipulation reduced the export of new or recycled TfRs
428 to the cell surface. An example of how protocols determine outcomes is the variation in the
429 measured half-life of TfR, which ranges from ~40 min to 7 hrs depending on the different
430 experimental protocols used (Biebinger et al., 2003; Kabiri & Steverding, 2000; Mussmann et
431 al., 2004; Tiengwe et al., 2017).
432
433 The experiments involving transferring BES1-VSG221 cells to medium in which FBS had
434 been replaced by canine serum (Mussmann et al., 2003) are informative. The BES1 TfR
435 does not bind canine transferrin and cell proliferation arrested. After ~5 days, proliferating
436 cells appeared in the culture having switched BES and thus TfR orthologue to one able to
437 bind canine transferrin (van Luenen et al., 2005). In addition, supplementing the canine
438 serum based medium with bovine transferrin prevented arrest of proliferation indicating that
439 it was due to lack of transferrin alone (Mussmann et al., 2004). In contrast to experiments
440 that wash cells into solutions that do not support growth, the transfer of BES1-VSG221 cells
441 to medium with canine serum starves the cells of just transferrin. On transfer from FBS to
442 canine serum, the TfR abundance increased 4 to 5-fold and the receptor was present all
443 over the cell surface (Mussmann et al., 2003). It is unlikely that the distribution of TfR on the
444 cell surface results from a retention system being overwhelmed given the variation in TfR
445 expression observed from different BESs (Figure 1) but is due to an absence of ligand-
446 mediated uptake. Different TfRs have a wide range of affinities for transferrins (K_D from as
447 low as 1.4 nM to >5 μM) (Trevor et al., 2019) and there will be an equilibrium with the
448 relative amounts of TfR on the cell body surface compared with the flagellar pocket and
449 internal structures that will vary with the identity of the TfR and the identity and concentration
450 of transferrin.
451
452 The experiments here were informed by the kinetics of rapid transferrin uptake (Figure 3 and
453 as an unpublished observation in (Mussmann et al., 2004) and we did not manipulate the
454 cells before ligand uptake experiments or prior to fixation for immunolocalization. The result
455 was clear evidence that TfR is expressed over the whole cell surface and is not restricted to
456 the flagellar pocket. This was reinforced by the localisation of the HpHbR and FHR, both of
457 which are monomeric (Lane-Serff et al., 2014; Macleod et al., 2020), contain a single GPI-
458 anchor, and are also present over the whole cell surface. We also observed variation in TfR

459 and HpHbR abundance between individual cells, as has been seen previously for TfR
460 (Duncan et al., 2024; Steverding et al., 1994b), and this suggests sensitivity to the
461 requirements at the individual cell level. Whether this relates to cell cycle stage or any
462 developmental progression remains to be investigated. The expression of the TfR is
463 sensitive to the availability of Fe^{3+} with a several fold increases in mRNA and protein induced
464 by iron chelators (Gilabert Carbajo et al., 2021). Growth in medium dependent on rabbit
465 serum resulted in high levels of expression of the FHR, this could result from a factor in
466 rabbit serum inducing expression or failure to bind ligand.
467
468 The findings here still leave the question of how the trypanosome avoids receptor antibody-
469 based clearance by the host immune system? Vaccination of mice with ISGs did not result in
470 any protection (Ziegelbauer & Overath, 1993), this shows that receptors do not have to be
471 sequestered in the flagellar pocket to avoid the host adaptive immune system. The effective
472 killing of trypanosomes by antibody-drug conjugates recognising the HpHbR shows that
473 receptors are accessible (MacGregor et al., 2019), as does inhibition of transferrin binding by
474 Fab fragments (Steverding et al., 1995). It is likely that a combination of processes results in
475 resistance to receptor antibody-mediated killing: first antibodies have to recognise parts of
476 the receptor that are accessible in the VSG coat, this will be affected by the structure of the
477 receptor and how much is occluded by ligand binding, a function of ligand concentrations,
478 host species and receptor K_D. Enough antibody has to be present on the cell surface for long
479 enough to elicit a response. Two factors affect this, first the copy number of the receptor,
480 ISGs are present at 50,000 to 70,000 per cell (Ziegelbauer et al., 1992) (<1% of VSG), TfR
481 at a few thousand, but variable (Steverding et al., 1995), and HpHbR at 300 to 400
482 (Vanhollebeke et al., 2008). Second, the half time of the receptor antibody complex on the
483 cell body plasma membrane will be short (Steverding et al., 1995) as the hydrodynamic
484 forces rapidly push VSG-antibody complexes toward the flagellar pocket and endocytosis
485 (Engstler et al., 2007). In summary, we provide evidence that GPI-anchored receptors in
486 trypanosomes are not sequestered in the flagellar pocket but are distributed across the cell
487 body and flagellum surface plasma membrane and this leads to re-evaluation of how
488 trypanosomes avoid receptor antibody mediated clearance.
489
490
491 **MATERIALS AND METHODS**
492
493 **Cell lines**

494 *T. brucei* Lister427 bloodstream form cell lines were used throughout expressing either
495 VSG221 (MiTat1.2) from BES1, VSG118 (MITat 1.5) from BES3 or VSG224 (MITat 1.3) from
496 BES7. BES7 expressing cells were as described in Hertz-Fowler *et al.* (Hertz-Fowler et al.,
497 2008) where BES1 and BES7 were tagged with Puromycin and G418 resistance genes
498 respectively. Cells were maintained in culture in HMI-11 medium (Hirumi & Hirumi, 1989).
499 For ligand-uptake assays and immunofluorescence cells were harvested in mid-log phase
500 (0.5-1x10^6 cells/ml). To allow further modification by (CRISPR)-associated gene 9 (Cas9)
501 gene editing, BES1 and BES7 expressing cell lines were first modified by transfection with a
502 construct containing Cas9 and T7 RNA polymerase transgenes (Beneke et al., 2017).
503 Antibiotic selection was used when appropriate. The primers used to generate the cell lines
504 are listed in Supplementary Table1.

505

506 **Constructs for ESAG7 +/- GPI attachment site**

507 Constructs are represented schematically in Figure 2A and described in brief below:

508 BES7 constructs:

509 The presence of a G418 resistance gene upstream of ESAG7 was utilised to generate the
510 required constructs from BES7 genomic DNA (Hertz-Fowler et al., 2008). A PacI-EcoRI PCR
511 fragment from the promoter to the G418 resistance gene start was annealed to an EcoRI-
512 PacI PCR fragment from the G418 stop codon through to the ESAG7 3' UTR. The resulting
513 EcoRI site was used to insert a blasticidin resistance open reading frame. The entire
514 construct was cloned into pGEM-T, allowing the required cassette to be excised by PacI for
515 transfection into BES7 cells expressing Cas9, alongside suitable sgRNAs to target the
516 BES7-ESAG7 region, designed by ChopChop (https://chopchop.cbu.uib.no/). This construct
517 contained the endogenous BES7 ESAG7 including its GPI anchor. To remove the GPI
518 anchor addition sequences and express an ESAG7 similar to those in the other Lister427
519 bloodstream expression sites, a SacI-BsrBI fragment was excised and replaced with the
520 corresponding fragment from BES1 ESAG7. This fragment was generated by RT-PCR from
521 RNA isolated from BES1 VSG221 cells using standard methods.

522 BES1 constructs:

523 A similar approach was used to make ESAG7 modifying constructs from BES1 exploiting a
524 puromycin resistance gene located between the promoter and the ESAG7 gene in the BES1
525 expression site (Hertz-Fowler et al., 2008). PacI-BstEII and BstEII-PacI PCR fragments were
526 generated from genomic DNA, ligated and cloned into pGEM-T. To generate BES1-ESAG7
527 with a GPI anchor from the BES1 expression site, the distal SacI-PacI fragment was

528 replaced by a PCR fragment encoding SacI-ESAG7 stop codon (blunt end) from BES7-
529 ESAG7 DNA and a BES1-ESAG7 3' UTR region from the BES1 site corresponding to the
530 BES7-ESAG7 stop codon (blunt end) to PacI. Constructs were linearised with PacI and
531 transfected with sgRNAs targeting the ESAG7 gene in either BES7 or BES1 and
532 electroporated into BES1 VSG221 cells expressing Cas9. BES7 modified cell lines were
533 selected with blasticidin and BES1 modified cell lines with puromycin.

534 Changing the VSG from 224 to 221:

535 BES7-VSG224 expression was switched to VSG221 by transfection of a linearised plasmid
536 fragment encoding VSG221, flanked by 5' and 3' VSG221 intergenic regions and a
537 downstream G418 resistance gene flanked by alpha-beta tubulin intergenic regions.
538 Sequences targeting the 5' and 3' UTRs of the endogenous VSG224 gene were generated
539 by PCR from BES7 (TAR153) DNA (a kind gift of Luísa Figueiredo) and cloned via KpnI/XhoI
540 and SpeI/SacI fragments upstream and downstream of the VSG221-blasticidin expression
541 cassette. G418 resistant clones were screened for binding to anti-VSG221 antibody through
542 immunofluorescence assays and confirmed by Western blot analysis.

543

544 **Protein gel electrophoresis and Western blotting**

545 Protein samples were prepared and analysed by SDS-PAGE and western blotting following
546 standard methods. Briefly, cells were harvested by centrifugation, washed in serum-free
547 HMI-9 and resuspended in Protein Sample Buffer (10% glycerol, 2% w/v SDS, 80 mM Tris-
548 HCl pH 6.8), at a concentration of $2x10^8$ cells/ml. Immobilon-P membrane (Millipore) was
549 used to retain the proteins. The primary antibodies used during western blotting are rabbit
550 anti-FHR (Macleod et al., 2020) and rabbit anti-TfR (a kind gift of Piet Borst). Polyclonal anti-
551 VSG221 and anti-SCD6 antibodies were generated from recombinant *E. coli* expressed
552 proteins, injected into rabbits by standard methods (Covalab). Secondary antibodies used
553 were Peroxidase-conjugated AffiniPure Goat Anti-Rabbit IgG (H+L) (Jackson
554 Immunoresearch) and Alexa Fluor 488-Donkey Anti-Rabbit IgG (H+L) (Invitrogen).
555 Membranes were blocked in Tris-buffered saline (TBS), 0.1% Tween20, 2% w/v Marvel dried
556 milk and probed in appropriate dilutions of primary and secondary antibodies. Washing steps
557 were performed with TBS, 0.1% Tween20 and blots were analysed on a BioRad ChemiDoc
558 system, ensuring signals remained below saturation limits. Quantitation of transferrin
559 receptor protein level was performed using Fiji-ImageJ software
560 (https://imagej.net/software/fiji/), with background subtraction and comparison with intensity
561 measurements taken from a protein dilution series from BES7 expressing cells.

562

563 **Ligand uptake**

564 Bovine holo-transferrin (ThermoFisher) was dialyzed against PBS and labelled with Alexa
565 fluor 568 NHS ester (ThermoFisher) following the manufacturer's protocol. Canine
566 transferrin was obtained from Abbexa and loaded with iron using a four-fold molar excess of
567 ammonium iron (III) sulphate in presence of 5 mM sodium bicarbonate followed by dialysis
568 against 10 mM HEPES pH 7.4, 150 mM NaCl as described previously (Trevor et al., 2019).
569 Canine holo- transferrin was then labelled with Alexa fluor 568 NHS ester (ThermoFisher) as
570 above. The Hp-Hb complex was purified as described (Lane-Serff et al., 2014) and labelled
571 with Alexa fluor 568 NHS ester (ThermoFisher) following the manufacturer's protocol.

572

573 Mid log-phase cells (~ 6 x 10^5 /ml) were supplemented with 500 nM Alexa 568 labelled ligand
574 and incubated at 37°C. At time points, cells were fixed by the addition of 8% formaldehyde in
575 PBS to a final concentration 1% and incubated for 5 min. Cells were further washed with
576 PBS plus 1% BSA and DNA was stained with Hoechst 33258. Slides were prepared and
577 images were captured within next within the next 30 min using Zeiss Axio Imager.Z2 with
578 X100 objective. Samples in any one experiment were excited with the same intensity and
579 using the same exposure time. Images were processed using the ZEN Blue software.

580

581 **Immunofluorescence localisation and microscopy**

582 *T. brucei* cells were fixed in culture by the addition of one volume of 8% formaldehyde, 0.4%
583 glutaraldehyde in PBS for 10 min. After fixation, cells were washed with serum free HMI-9
584 plus 1% bovine serum albumin (BSA) twice and immobilized on poly-lysine coated slides for
585 1 hr. Immobilized cells were treated with 0.1% triton X-100 (in PBS) for 5 min , washed with
586 PBS and then incubated with PBS, 1% BSA for 10 min. Cells were incubated with the rabbit
587 anti-TfR (1:50) or anti- FHR (Macleod et al., 2020) (1:50) in PBS, 1% BSA for 1 hr, washed
588 three times with PBS and then with donkey anti- rabbit Alexa488 (1:800) in PBS, 1% BSA for
589 1 hr. Cells were washed three times with PBS and the last wash contained 0.1 µg/ml
590 Hoechst 33258 to stain DNA. Cells were mounted with anti-fade and were visualized under
591 Zeiss Axio Imager.Z2 with X100 objective. In any one experiment, samples were illuminated
592 with same exposure time, intensity for respective excitation channels. All
593 immunofluorescence experiments were repeated three to six times with similar results. The
594 images were processed with ZEN Blue software by adjusting the brightness and contrast
595 with the same changes being made to all images in any one experiment including the
596 negative controls.

597 Measurements of the fluorescence intensity of ligands or receptor antibodies in individual
598 cells was performed using the ZEN Blue software. Mean fluorescence intensity was
599 measured and background fluorescence intensity was subtracted. ImageJ software was
600 used to measure the point fluorescence intensity of ligands and receptor antibodies by
601 drawing a line perpendicular to the long axis of the cell, and the distribution profile against
602 the distance was plotted. For 3D structured illumination, a Zeiss Elyra7 microscope with X63
603 objective was used in the Cambridge Advanced Imaging Centre. Slides were prepared as
604 above and the processing of all images and the 3D reconstruction were performed with ZEN
605 Blue software only by adjusting the brightness contrast.

606

607 **FIGURE LEGENDS**

608

609 **Figure 1. *T. brucei* transferrin receptor expressed from BES7 contains GPI-anchored**
610 **ESAG7.**
611 (A) Phylogenetic tree showing the relationship between ESAG6 and ESAG7 proteins from *T.*
612 *brucei* Lister 427 (Hertz-Fowler et al., 2008). The tree was assembled in Geneious Prime
613 (www.geneious.com) using an alignment by Muscle 5.1 followed by a neighbour joining tree
614 with 100 bootstraps and no outgroup on residues 1 to 332 of the alignment. BES7 ESAG 6
615 and 7 are shown in red.
616 (B) Variation in transferrin receptor expression in cell lines expressing VSGs from different
617 bloodstream form expression sites (BES). BES3-VSG118, BES1-VSG221, BES7-VSG224
618 cell lines are unmanipulated and the BES7-VSG221 was made after exchanging VSG224 for
619 VSG221 (see Figure 2A). Cell lysates were treated with PNGaseF and 2 x 10^6 cells
620 equivalents were loaded. Western blots were probed with anti-TfR, and then overprobed with
621 anti-VSG221. ESAG6 and ESAG7 plus GPI-anchor variants are indicated; BES3-VSG118
622 and BES1-VSG221 cell lysates contain ESAG7 without the GPI anchor. BES3-VSG118 and
623 BES7-VSG224 cell lysates did not show any VSG221. The presence of VSG221 protein
624 confirmed the switching of BES7 VSG224 to VSG221. Switching in VSG type did not affect
625 the expression pattern of native TfR (ESAG6/7 plus GPI) protein. Coomassie blue stained
626 SDS-PAGE gel to demonstrate loading of samples.

627

628 **Figure 2. BES identity and the number of GPI-anchors determines the cellular TfR**
629 **levels.**
630 (A) Schematic illustrating the production of cell lines. For the addition and removal of ESAG7
631 GPI-anchor addition sequences, two constructs were used for each of BES1 and BES7. A
632 description of the construct is provided in the methods. For BES7, the same process was

633 used, one construct removing the GPI-anchor from ESAG7, the other leaving it intact. For
634 BES1, integration of one resulted in modification of ESAG7 to add a GPI-anchor, integration
635 of the second resulted in an unchanged ESAG7 polypeptide sequence. Restriction enzyme
636 sites used in cloning: P, PacI; E, EcoRI; S, SacI; Bs, BstEII and Bb, BsrBI. The VSG in
637 BES7-VSG224 cells was switched to VSG221 to remove any VSG-dependent variation. The
638 targeting construct conferred G418 resistance. (B) Transferrin receptor expression in the
639 following cell lines: BES7-VSG221 single (1-GPI) and double (2-GPI) GPI-anchored TfR and
640 BES1-VSG221 single and double GPI-anchored TfR. Cell lysates were treated with
641 PNGaseF and 2 x 10^6 cells equivalents were loaded per gel track. A western blot of the
642 samples was probed with anti-TfR then over probed with anti-VSG221 and anti-SCD6.
643 ESAG6 and ESAG7 plus GPI-anchor variants are indicated.
644 (C) TfR quantitation estimates from a minimum of three biological replicates of each cell line,
645 error bars display the standard deviation for each sample. Samples plus a dilution series
646 from BES7-221 were minimally separated by SDS-PAGE to compress TfR components to a
647 single band for analysis after western blotting, probed with anti-TfR and anti-SCD6. Donkey
648 anti-rabbit Alexa 488 was used as secondary antibody and band intensity was calculated by
649 ImageJ ensuring that signals taken for each reading were below saturation levels. Relative
650 quantitation was determined by mapping values to those obtained from a dilution series.
651 Measurements for SDC6 were used to normalise cell loading with the value for BES1-1GPI
652 anchor samples given an arbitrary value of 1. Statistical analysis was used a two-tailed
653 paired t-test, $**p \leq 0.01$; $*p \leq 0.05$.
654
655 **Figure 3. Transferrin endocytosis is rapid, in both single and double GPI-anchored**
656 **cells. Initial binding is to the cell surface and internalization is detected within 60 sec.**
657 Cultures of single (1-GPI) or double (2-GPI) GPI-anchored TfR expressing BES7-VSG221
658 and BES1-VSG221 cells were supplemented with 500 nM Alexa568 labelled holo- transferrin
659 (Tf_{A568}) and incubated for 15 sec, 60 sec or 600 sec and fixed by addition of formaldehyde to
660 1% for 5 min. Following washing with PBS containing 1% bovine serum albumin cells were
661 visualized under Zeiss Axio Imager.Z2 with X100 objective. Images in all these experimental
662 time points for both 1- and 2GPI TfR cells were captured with same intensity of excitation
663 and exposure time.
664 (A) Images showing the location of bound or endocytosed transferrin in representative cells
665 in populations and at time points as indicated. Scale bar is 5 μm. Images were processed
666 with ZEN Blue 3.4 software without any deconvolution. Larger numbers of cells are shown in
667 Supplementary Figure 3.
668 (B) The variation between individual cells in transferrin binding and uptake and endocytosis
669 shown by measurements of total fluorescence intensity of Tf_{A568} in BES7 VSG221 1- and 2-

670 GPI TfR cells at 15 sec, 60 sec and 600 sec. Measurements were obtained using Zen Blue
671 3.4 software and normalizing the background fluorescence. Scatter plots of measurements
672 of individual cells are shown for 1-GPI (grey) and 2-GPI (purple) TfRs. The average and
673 standard deviation are shown for each cell line**.**
674 (C) Tf_{A568} fluorescence intensity distribution across transverse sections of randomly selected
675 cells was measured using ImageJ software. The plots are shown for both BES7 1- and 2-
676 GPI cell lines, showing the pattern of individual cells in different colours at 60 sec and 600
677 sec.
678 (D) (E) and (F) Same as (A) (B) and (C) but with BES1-VSG221 1- and 2GPI TfR expressing
679 cells.
680
681 **Figure 4. Immunofluorescence localisation of single and double GPI-anchored**
682 **transferrin receptors to the entire plasma membrane.**
683 Cell lines expressing VSG221 and either 1- or 2-GPI TfR variants were fixed in culture with
684 final concentrations of 4% formaldehyde and 0.2% glutaraldehyde. Immunofluorescence
685 localisations were performed with rabbit anti-TfR followed by donkey anti-rabbit Alexa 488
686 (green). Cells were visualized using a Zeiss Axio Imager.Z2 with X100 objective. Images in
687 all these experimental sets were captured with same intensity of excitation and exposure
688 time.
689 (A) Localization in cell lines as indicated. Scale bar is 5 µm. Images were processed with
690 ZEN Blue 3.4 software. A larger number of cells is shown in Supp. Figure 5.
691 (B) Fluorescence distribution across transverse sections of the cells was measured using
692 ImageJ software. Plots are shown for both BES7-VSG221 TfR cell lines, each cell in a
693 different colour.
694 (C) Mean anti-TfR fluorescence intensity in individual cells of both BES1 VSG221 and BES7
695 VSG221 1- and 2-GPI TfR cell population was measured using ZEN Blue 3.4 and
696 normalized against the background fluorescence. Bar diagram shows the fluorescence
697 intensity of either 1-GPI (grey) or 2-GPI (purple) TfR from individual cells. The columns
698 represent the average and the error bars show the standard deviation.
699
700 **Figure 5. Localization of single and double GPI-anchored transferrin receptors under**
701 **3D structured illumination microscope.**
702 Cells expressing either 1- or 2-GPI-anchored TfR were fixed in culture with final
703 concentrations of 4% formaldehyde and 0.2% glutaraldehyde. Immunofluorescence
704 localisation was performed with rabbit anti-TfR and donkey anti-rabbit Alexa 488. Cells were
705 visualized using a Zeiss Elyra7 microscope with X63 objective. Images in all these

706 experimental sets were captured with same intensity of excitation and exposure time. (A)
707 Localization of TfR in different cell lines as indicated. Scale bar is 5 µm.
708 (B) 3D projection generated using ZEN Blue 3.4 software example cells from the cell lines as
709 indicated. These images show the localization pattern of TfR on the cell surface as well as
710 within intracellular compartments. X-Y-Z axis is indicated.
711
712 **Figure 6. Haptoglobin-haemoglobin endocytosis assay. Initial binding is to the cell**
713 **surface followed by rapid endocytosis.**
714 Cells were supplemented with 500 nM Alexa 568 labelled HpHb, incubated for 15 sec, 60
715 sec or 600 sec and fixed in culture with 1% formaldehyde. Following washing with PBS
716 containing 1% bovine serum albumin. Cells were visualized under Zeiss Axio Imager.Z2 with
717 x100 objective. Images in all these experimental time points were captured with same
718 excitation intensity and exposure time.
719 (A) Images showing the location of HpHb in +/+ and -/- cells at different time points in
720 representative cells as indicated. Images were processed with ZEN Blue 3.4 software. Scale
721 bar is 5 µm. A greater number of cells is shown in Supp. Figure 6.
722 (B) HpHb fluorescence intensity distribution over transverse section of cells at 15 sec
723 measured using ImageJ software. Individual cells are shown in different colours.
724
725 **Figure 7. The complement factor H receptor localises to the cell surface.**
726 The observation that abundant FHR expression occurred in cells grown in rabbit serum but
727 not in FBS supplemented medium was used to investigate its localisation.
728 (A) Western blot analysis of FHR expression in *T. brucei* EATRO1125 cells grown in medium
729 supplemented with either foetal bovine serum or rabbit serum. Cell lysates were not treated
730 with PNGaseF and $2x10^6$ cells equivalent were loaded. The blot was probed with rabbit anti-
731 FHR and then overprobed with anti-SCD6 for loading.
732 (B) Immunofluorescence determination of localisation of FHR in cell lines as indicated. Cells
733 were fixed in culture with final concentration of 4% formaldehyde and 0.2% glutaraldehyde.
734 Rabbit anti-FHR antibody was followed by donkey anti-rabbit Alexa 488 secondary antibody.
735 A set of cells grown in RbS, fixed similarly and stained only with secondary antibody was
736 used as a control for residual rabbit IgG from the growth medium and cells grown in FBS for
737 non-expressers. Cells were visualized using a Zeiss Axio Imager.Z2 with x100 objective.
738 Scale bar is 5 µm. A larger number of cells is shown in Supp. Figure 7
739 (C) Localisation of FHR by 3D structured illumination microscopy. Cells fixed as above were
740 visualised using a Zeiss Elyra7 with x63 objective. Images were processed with ZEN Blue
741 3.4 software. Two representative cells images showing FHR in white and merged panel with
742 DNA in blue. Scale bar is 5 µm.

743

744 **SUPPLEMENTARY FIGURE LEGENDS**

745

746 **Supp Figure 1. Relationship between ESAG7 variants.**

747 A. Clustal W alignment of the nucleotide sequences of ESAG7s showing the translation
748 termination codon in red. The sequence for GPI-addition is present in all genes but a series
749 of small deletions between nucleotides 980 and 1080 resulted in a frame shift and a new
750 stop codon that effectively removed the C-terminal ~50 residues from the open reading
751 frame.

752 B. Same alignment but just including ESAG7 from BES1 and BES7 showing the
753 conservation of the coding potential to the 3' side of the stop codon in BES1 ESAG7
754 indicating the shorter ESAG7 genes probably arose from a longer BES7-like variant.
755 Functional stop codons are in red.

756

757 **Supp Figure 2. Relationship between ESAG 6 and 7.**

758 Clustal W alignment of BES7 ESAG6 and 7 nascent polypeptide sequences. Predicted
759 processing sites are indicated by yellow highlighting. The N-terminal signal sequence
760 cleavage site was predicted using SignalP 6.0 and GPI-anchor addition sites by NetGPI 1.1
761 as detailed below the alignment.

762

763 **Supp Figure 3. Transferrin endocytosis is rapid, in both single and double GPI-**
764 **anchored cells. Initial binding is to the cell surface and internalization is detected**
765 **within 60 sec.**

766 Larger fields of cells from the experiments shown in Figure 3. Scale bar is 20 μm.

767

768 **Supp Figure 4. *T. brucei* BES7 VSG221 1- and 2-GPI transferrin receptor does not bind**
769 **canine transferrin.**

770 (A) Clustal W alignment of the polypeptide sequences of cow and dog transferrin.

771 (B) Cultures were supplemented with 500 nM Alexa568 labelled canine holo- transferrin and
772 incubated for 60 sec and fixed in culture by addition of formaldehyde to 1%. Following
773 washing with PBS containing 1% bovine serum albumin cells were visualized under Zeiss
774 Axio Imager.Z2 with x100 objective. Images for both BES7 VSG221 1- and 2-GPI TfR cells
775 were captured with same intensity of excitation and exposure time.

776 Images showing the absence of any bound or endocytosed canine transferrin in around forty
777 cells in population of both 1- and 2GPI TfR cells. Scale bar is 20 μm. Images were
778 processed ZEN Blue 3.4 software.

Supp Figure 5. Immunofluorescence localisation of single and double GPI-anchored transferrin receptors to the entire plasma membrane.

Larger fields of cells from the experiments shown in Figure 4. Scale bar is 20 µm.

Supp Figure 6. Haptoglobin-haemoglobin endocytosis assay. Initial binding is to the cell surface followed by rapid endocytosis.

Larger fields of cells from the experiments shown in Figure 6. Scale bar is 20 µm.

Supp Figure 7. The complement factor H receptor localises to the cell surface.

Larger fields of cells from the experiments shown in Figure 7B. Scale bar is 20 µm.

ACKNOWLEDGEMENTS

We would like to thank: Luísa Figueiredo for the gift of the cell line expressing VSG224 from BES7 and a BES7 TAR clone; Piet Borst for the transferrin receptor antibodies; Jay Bangs for a lot of fun discussions.

FUNDING

MC and MH are Wellcome Investigators (MC, 217138/Z/19/Z; MH, 220797/Z/20/Z). Initial funding for SB was from the Newton-Bhabha Fund.

References:

Banerjee, S., Minshall, N., Webb, H., & Carrington, M. (2024). How are Trypanosoma brucei receptors protected from host antibody-mediated attack? *BioEssays : News and Reviews in Molecular, Cellular and Developmental Biology*, e2400053. https://doi.org/10.1002/bies.202400053

Bangs, J. D., Andrews, N. W., Hart, G. W., & Englund, P. T. (1986). Posttranslational modification and intracellular transport of a trypanosome variant surface glycoprotein. *The Journal of Cell Biology*, *103*(1), 255–263. https://doi.org/10.1083/jcb.103.1.255

Barcons-Simon, A., Carrington, M., & Siegel, T. N. (2023). Decoding the impact of nuclear organization on antigenic variation in parasites. *Nature Microbiology*, *8*(8), 1408–1418. https://doi.org/10.1038/s41564-023-01424-9

Beneke, T., Madden, R., Makin, L., Valli, J., Sunter, J., & Gluenz, E. (2017). A CRISPR Cas9 high-throughput genome editing toolkit for kinetoplastids. *Royal Society Open Science*, *4*(5), 170095. https://doi.org/10.1098/rsos.170095

814 Biebinger, S., Helfert, S., Steverding, D., Ansorge, I., & Clayton, C. (2003). Impaired
815 dimerization and trafficking of ESAG6 lacking a glycosyl-phosphatidylinositol anchor.
816 *Molecular and Biochemical Parasitology*, *132*(2), 93–96.
817 https://doi.org/10.1016/j.molbiopara.2003.07.005

818 Bonhivers, M., Nowacki, S., Landrein, N., & Robinson, D. R. (2008). Biogenesis of the
819 trypanosome endo-exocytotic organelle is cytoskeleton mediated. *PLoS Biology*, *6*(5),
820 e105. https://doi.org/10.1371/journal.pbio.0060105

821 Chaudhri, M., Steverding, D., Kittelberger, D., Tjia, S., & Overath, P. (1994). Expression of a
822 glycosylphosphatidylinositol-anchored Trypanosoma brucei transferrin-binding protein
823 complex in insect cells. *Proceedings of the National Academy of Sciences of the United*
824 *States of America*, *91*(14), 6443–6447. https://doi.org/10.1073/pnas.91.14.6443

825 Cook, A. D., Carrington, M., & Higgins, M. K. (2024). Molecular mechanism of complement
826 inhibition by the trypanosome receptor ISG65. *ELife*, *12*.
827 https://doi.org/10.7554/eLife.88960

828 Duncan, S. M., Carbajo, C. G., Nagar, R., Zhong, Q., Breen, C., Ferguson, M. A. J., &
829 Tiengwe, C. (2024). Generation of a bloodstream form Trypanosoma brucei double
830 glycosyltransferase null mutant competent in receptor-mediated endocytosis of
831 transferrin. *PLoS Pathogens*, *20*(6), e1012333.
832 https://doi.org/10.1371/journal.ppat.1012333

833 Engstler, M., Pfohl, T., Herminghaus, S., Boshart, M., Wiegertjes, G., Heddergott, N., &
834 Overath, P. (2007). Hydrodynamic flow-mediated protein sorting on the cell surface of
835 trypanosomes. *Cell*, *131*(3), 505–515. https://doi.org/10.1016/j.cell.2007.08.046

836 Engstler, M., Thilo, L., Weise, F., Grünfelder, C. G., Schwarz, H., Boshart, M., & Overath, P.
837 (2004). Kinetics of endocytosis and recycling of the GPI-anchored variant surface
838 glycoprotein in Trypanosoma brucei. *Journal of Cell Science*, *117*(Pt 7), 1105–1115.
839 https://doi.org/10.1242/jcs.00938

840 Gadelha, C., Rothery, S., Morphew, M., McIntosh, J. R., Severs, N. J., & Gull, K. (2009).
841 Membrane domains and flagellar pocket boundaries are influenced by the cytoskeleton
842 in African trypanosomes. *Proceedings of the National Academy of Sciences of the*
843 *United States of America*, *106*(41), 17425–17430.
844 https://doi.org/10.1073/pnas.0909289106

845 Gadelha, C., Zhang, W., Chamberlain, J. W., Chait, B. T., Wickstead, B., & Field, M. C.
846 (2015). Architecture of a Host-Parasite Interface: Complex Targeting Mechanisms
847 Revealed Through Proteomics. *Molecular & Cellular Proteomics : MCP*, *14*(7), 1911–
848 1926. https://doi.org/10.1074/mcp.M114.047647

849 Gerrits, H., Mussmann, R., Bitter, W., Kieft, R., & Borst, P. (2002). The physiological
850 significance of transferrin receptor variations in Trypanosoma brucei. *Molecular and*
851 *Biochemical Parasitology*, *119*(2), 237–247. https://doi.org/10.1016/s0166-
852 6851(01)00417-0

853 Gilabert Carbajo, C., Cornell, L. J., Madbouly, Y., Lai, Z., Yates, P. A., Tinti, M., & Tiengwe, C.
854 (2021). Novel aspects of iron homeostasis in pathogenic bloodstream form
855 Trypanosoma brucei. *PLoS Pathogens*, *17*(6), e1009696.
856 https://doi.org/10.1371/journal.ppat.1009696

857 Gíslason, M. H., Nielsen, H., Almagro Armenteros, J. J., & Johansen, A. R. (2021).
858 Prediction of GPI-anchored proteins with pointer neural networks. *Current Research in*
859 *Biotechnology*, *3*, 6–13. https://doi.org/10.1016/j.crbiot.2021.01.001

860 Hertz-Fowler, C., Figueiredo, L. M., Quail, M. A., Becker, M., Jackson, A., Bason, N., Brooks,
861 K., Churcher, C., Fahkro, S., Goodhead, I., Heath, P., Kartvelishvili, M., Mungall, K.,
862 Harris, D., Hauser, H., Sanders, M., Saunders, D., Seeger, K., Sharp, S., … Berriman,
863 M. (2008). Telomeric expression sites are highly conserved in Trypanosoma brucei.
864 *PloS One*, *3*(10), e3527. https://doi.org/10.1371/journal.pone.0003527

865 Higgins, M. K., Tkachenko, O., Brown, A., Reed, J., Raper, J., & Carrington, M. (2013).
866 Structure of the trypanosome haptoglobin-hemoglobin receptor and implications for
867 nutrient uptake and innate immunity. *Proceedings of the National Academy of Sciences*
868 *of the United States of America*, *110*(5), 1905–1910.
869 https://doi.org/10.1073/pnas.1214943110

870 Hirumi, H., & Hirumi, K. (1989). Continuous cultivation of Trypanosoma brucei blood stream
871 forms in a medium containing a low concentration of serum protein without feeder cell
872 layers. *The Journal of Parasitology*, *75*(6), 985–989.

873 Hsia, R., Beals, T., & Boothroyd, J. C. (1996). Use of chimeric recombinant polypeptides to
874 analyse conformational, surface epitopes on trypanosome variant surface
875 glycoproteins. *Molecular Microbiology*, *19*(1), 53–63. https://doi.org/10.1046/j.1365-
876 2958.1996.351878.x

877 Kabiri, M., & Steverding, D. (2000). Studies on the recycling of the transferrin receptor in
878 Trypanosoma brucei using an inducible gene expression system. *European Journal of*
879 *Biochemistry*, *267*(11), 3309–3314. https://doi.org/10.1046/j.1432-1327.2000.01361.x

880 Kakuta, K., Orino, K., Yamamoto, S., & Watanabe, K. (1997). High levels of ferritin and its
881 iron in fetal bovine serum. *Comparative Biochemistry and Physiology. Part A,*
882 *Physiology*, *118*(1), 165–169. https://doi.org/10.1016/s0300-9629(96)00403-3

883 Lane-Serff, H., MacGregor, P., Lowe, E. D., Carrington, M., & Higgins, M. K. (2014).
884 Structural basis for ligand and innate immunity factor uptake by the trypanosome
885 haptoglobin-haemoglobin receptor. *ELife*, *3*, e05553.
886 https://doi.org/10.7554/eLife.05553

887 Lane-Serff, H., MacGregor, P., Peacock, L., Macleod, O. J., Kay, C., Gibson, W., Higgins, M.
888 K., & Carrington, M. (2016). Evolutionary diversification of the trypanosome
889 haptoglobin-haemoglobin receptor from an ancestral haemoglobin receptor. *ELife*, *5*.
890 https://doi.org/10.7554/eLife.13044

891 Leung, K. F., Riley, F. S., Carrington, M., & Field, M. C. (2011). Ubiquitylation and
892 developmental regulation of invariant surface protein expression in trypanosomes.
893 *Eukaryotic Cell*, *10*(7), 916–931. https://doi.org/10.1128/EC.05012-11

894 Ligtenberg, M. J., Bitter, W., Kieft, R., Steverding, D., Janssen, H., Calafat, J., & Borst, P.
895 (1994). Reconstitution of a surface transferrin binding complex in insect form
896 Trypanosoma brucei. *The EMBO Journal*, *13*(11), 2565–2573.
897 https://doi.org/10.1002/j.1460-2075.1994.tb06546.x

898 MacGregor, P., Gonzalez-Munoz, A. L., Jobe, F., Taylor, M. C., Rust, S., Sandercock, A. M.,
899 Macleod, O. J. S., Van Bocxlaer, K., Francisco, A. F., D'Hooge, F., Tiberghien, A., Barry,
900 C. S., Howard, P., Higgins, M. K., Vaughan, T. J., Minter, R., & Carrington, M. (2019). A

single dose of antibody-drug conjugate cures a stage 1 model of African trypanosomiasis. *PLoS Neglected Tropical Diseases*, *13*(5), e0007373. https://doi.org/10.1371/journal.pntd.0007373

Macleod, O. J. S., Bart, J.-M., MacGregor, P., Peacock, L., Savill, N. J., Hester, S., Ravel, S., Sunter, J. D., Trevor, C., Rust, S., Vaughan, T. J., Minter, R., Mohammed, S., Gibson, W., Taylor, M. C., Higgins, M. K., & Carrington, M. (2020). A receptor for the complement regulator factor H increases transmission of trypanosomes to tsetse flies. *Nature Communications*, *11*(1), 1326. https://doi.org/10.1038/s41467-020-15125-y

Macleod, O. J. S., Cook, A. D., Webb, H., Crow, M., Burns, R., Redpath, M., Seisenberger, S., Trevor, C. E., Peacock, L., Schwede, A., Kimblin, N., Francisco, A. F., Pepperl, J., Rust, S., Voorheis, P., Gibson, W., Taylor, M. C., Higgins, M. K., & Carrington, M. (2022). Invariant surface glycoprotein 65 of Trypanosoma brucei is a complement C3 receptor. *Nature Communications*, *13*(1), 5085. https://doi.org/10.1038/s41467-022-32728-9

Maier, A., & Steverding, D. (2008). Expression and purification of non-glycosylated Trypanosoma brucei transferrin receptor in insect cells. *Experimental Parasitology*, *120*(2), 205–207. https://doi.org/10.1016/j.exppara.2008.07.004

Mikkelsen, J. H., Stødkilde, K., Jensen, M. P., Hansen, A. G., Wu, Q., Lorentzen, J., Graversen, J. H., Andersen, G. R., Fenton, R. A., Etzerodt, A., Thiel, S., & Andersen, C. B. F. (2024). Trypanosoma brucei Invariant Surface Glycoprotein 75 Is an Immunoglobulin Fc Receptor Inhibiting Complement Activation and Antibody-Mediated Cellular Phagocytosis. *Journal of Immunology (Baltimore, Md. : 1950)*, *212*(8), 1334–1344. https://doi.org/10.4049/jimmunol.2300862

Mugnier, M. R., Cross, G. A. M., & Papavasiliou, F. N. (2015). The in vivo dynamics of antigenic variation in Trypanosoma brucei. *Science (New York, N.Y.)*, *347*(6229), 1470–1473. https://doi.org/10.1126/science.aaa4502

Mussmann, R., Engstler, M., Gerrits, H., Kieft, R., Toaldo, C. B., Onderwater, J., Koerten, H., van Luenen, H. G. A. M., & Borst, P. (2004). Factors affecting the level and localization of the transferrin receptor in Trypanosoma brucei. *The Journal of Biological Chemistry*, *279*(39), 40690–40698. https://doi.org/10.1074/jbc.M404697200

Mussmann, R., Janssen, H., Calafat, J., Engstler, M., Ansorge, I., Clayton, C., & Borst, P. (2003). The expression level determines the surface distribution of the transferrin receptor in Trypanosoma brucei. *Molecular Microbiology*, *47*(1), 23–35. https://doi.org/10.1046/j.1365-2958.2003.03245.x

Pays, E., Lips, S., Nolan, D., Vanhamme, L., & Pérez-Morga, D. (2001). The VSG expression sites of Trypanosoma brucei: multipurpose tools for the adaptation of the parasite to mammalian hosts. *Molecular and Biochemical Parasitology*, *114*(1), 1–16. https://doi.org/10.1016/s0166-6851(01)00242-0

Pinger, J., Nešić, D., Ali, L., Aresta-Branco, F., Lilic, M., Chowdhury, S., Kim, H.-S., Verdi, J., Raper, J., Ferguson, M. A. J., Papavasiliou, F. N., & Stebbins, C. E. (2018). African trypanosomes evade immune clearance by O-glycosylation of the VSG surface coat. *Nature Microbiology*, *3*(8), 932–938. https://doi.org/10.1038/s41564-018-0187-6

Redpath, M. B., Windle, H., Nolan, D., Pays, E., Voorheis, H. P., & Carrington, M. (2000). ESAG11, a new VSG expression site-associated gene from Trypanosoma brucei.

945 *Molecular and Biochemical Parasitology*, *111*(1), 223–228.
946 https://doi.org/10.1016/s0166-6851(00)00305-4

947 Roggy, J. L., & Bangs, J. D. (1999). Molecular cloning and biochemical characterization of a
948 VCP homolog in African trypanosomes. *Molecular and Biochemical Parasitology*, *98*(1),
949 1–15. https://doi.org/10.1016/s0166-6851(98)00114-5

950 Salmon, D., Geuskens, M., Hanocq, F., Hanocq-Quertier, J., Nolan, D., Ruben, L., & Pays,
951 E. (1994a). A novel heterodimeric transferrin receptor encoded by a pair of VSG
952 expression site-associated genes in T. brucei. *Cell*, *78*(1), 75–86.
953 https://doi.org/10.1016/0092-8674(94)90574-6

954 Salmon, D., Geuskens, M., Hanocq, F., Hanocq-Quertier, J., Nolan, D., Ruben, L., & Pays,
955 E. (1994b). A novel heterodimeric transferrin receptor encoded by a pair of VSG
956 expression site-associated genes in T. brucei. *Cell*, *78*(1), 75–86.
957 https://doi.org/10.1016/0092-8674(94)90574-6

958 Schwartz, K. J., Peck, R. F., Tazeh, N. N., & Bangs, J. D. (2005). GPI valence and the fate of
959 secretory membrane proteins in African trypanosomes. *Journal of Cell Science*, *118*(Pt
960 23), 5499–5511. https://doi.org/10.1242/jcs.02667

961 Schwede, A., Jones, N., Engstler, M., & Carrington, M. (2011). The VSG C-terminal domain
962 is inaccessible to antibodies on live trypanosomes. *Molecular and Biochemical*
963 *Parasitology*, *175*(2), 201–204. https://doi.org/10.1016/j.molbiopara.2010.11.004

964 Steverding, D., Stierhof, Y. D., Chaudhri, M., Ligtenberg, M., Schell, D., Beck-Sickinger, A.
965 G., & Overath, P. (1994a). ESAG 6 and 7 products of Trypanosoma brucei form a
966 transferrin binding protein complex. *European Journal of Cell Biology*, *64*(1), 78–87.

967 Steverding, D., Stierhof, Y. D., Chaudhri, M., Ligtenberg, M., Schell, D., Beck-Sickinger, A.
968 G., & Overath, P. (1994b). ESAG 6 and 7 products of Trypanosoma brucei form a
969 transferrin binding protein complex. *European Journal of Cell Biology*, *64*(1), 78–87.

970 Steverding, D., Stierhof, Y. D., Fuchs, H., Tauber, R., & Overath, P. (1995). Transferrin-
971 binding protein complex is the receptor for transferrin uptake in Trypanosoma brucei.
972 *The Journal of Cell Biology*, *131*(5), 1173–1182. https://doi.org/10.1083/jcb.131.5.1173

973 Tiengwe, C., Bush, P. J., & Bangs, J. D. (2017). Controlling transferrin receptor trafficking
974 with GPI-valence in bloodstream stage African trypanosomes. *PLoS Pathogens*, *13*(5),
975 e1006366. https://doi.org/10.1371/journal.ppat.1006366

976 Trevor, C. E., Gonzalez-Munoz, A. L., Macleod, O. J. S., Woodcock, P. G., Rust, S.,
977 Vaughan, T. J., Garman, E. F., Minter, R., Carrington, M., & Higgins, M. K. (2019).
978 Structure of the trypanosome transferrin receptor reveals mechanisms of ligand
979 recognition and immune evasion. *Nature Microbiology*, *4*(12), 2074–2081.
980 https://doi.org/10.1038/s41564-019-0589-0

981 van Luenen, H. G. A. M., Kieft, R., Mussmann, R., Engstler, M., ter Riet, B., & Borst, P.
982 (2005). Trypanosomes change their transferrin receptor expression to allow effective
983 uptake of host transferrin. *Molecular Microbiology*, *58*(1), 151–165.
984 https://doi.org/10.1111/j.1365-2958.2005.04831.x

985 Vanhollebeke, B., De Muylder, G., Nielsen, M. J., Pays, A., Tebabi, P., Dieu, M., Raes, M.,
986 Moestrup, S. K., & Pays, E. (2008). A haptoglobin-hemoglobin receptor conveys innate
987 immunity to Trypanosoma brucei in humans. *Science (New York, N.Y.)*, *320*(5876),
988 677–681. https://doi.org/10.1126/science.1156296

Ziegelbauer, K., Multhaup, G., & Overath, P. (1992). Molecular characterization of two invariant surface glycoproteins specific for the bloodstream stage of Trypanosoma brucei. *The Journal of Biological Chemistry*, *267*(15), 10797–10803.

Ziegelbauer, K., & Overath, P. (1992). Identification of invariant surface glycoproteins in the bloodstream stage of Trypanosoma brucei. *The Journal of Biological Chemistry*, *267*(15), 10791–10796.

Ziegelbauer, K., & Overath, P. (1993). Organization of two invariant surface glycoproteins in the surface coat of Trypanosoma brucei. *Infection and Immunity*, *61*(11), 4540–4545. https://doi.org/10.1128/iai.61.11.4540-4545.1993

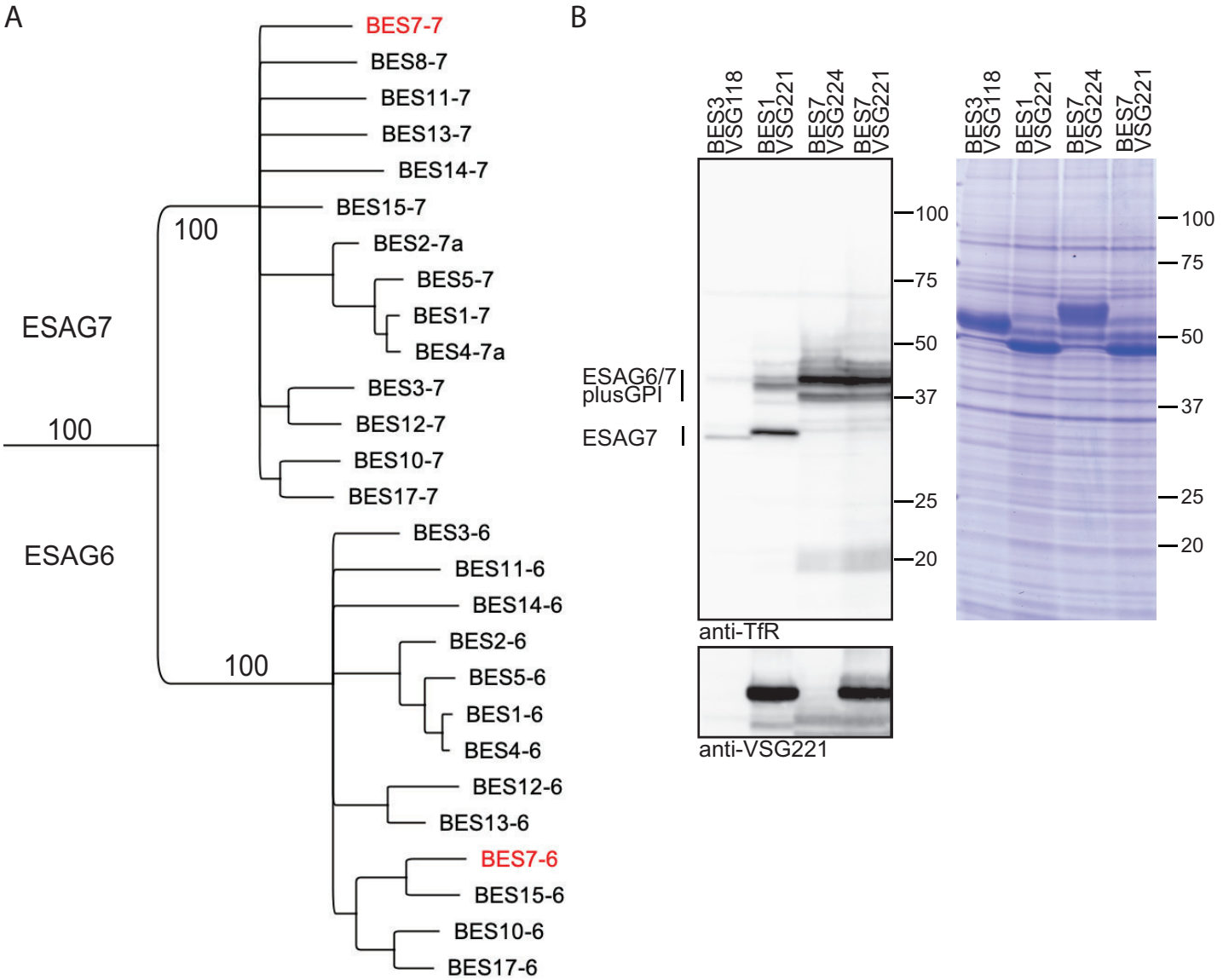
A
BES7-7
BES8-7
BES11-7
BES13-7
BES14-7
BES15-7
100
BES2-7a
BES5-7
BES1-7
BES4-7a
ESAG7
BES3-7
100
BES12-7
BES10-7
BES17-7
ESAG6
BES3-6
BES11-6
BES14-6
BES2-6
100
BES5-6
BES1-6
BES4-6
BES12-6
BES13-6
BES7-6
BES15-6
BES10-6
BES17-6
B
BES3 VSG118
BES1 VSG221
BES7 VSG224
BES7 VSG221
ESAG6/7 plusGPI
ESAG7
100
75
50
37
25
20
anti-TfR
anti-VSG221
BES3 VSG118
BES1 VSG221
BES7 VSG224
BES7 VSG221
100
75
50
37
25
20

Figure 1

A

Changes to BES7 ESAG7

altered anchor construct

ESAG6/7 genomic locus

unchanged anchor construct

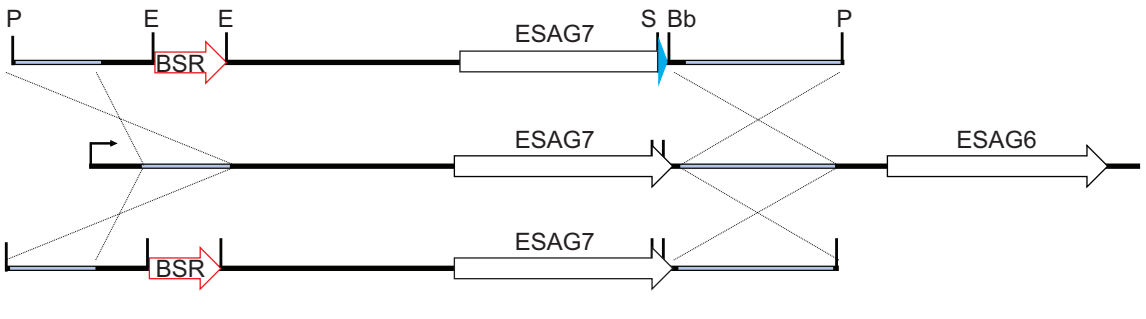

Changes to BES1 ESAG7

altered anchor construct

ESAG6/7 genomic locus

unchanged anchor construct

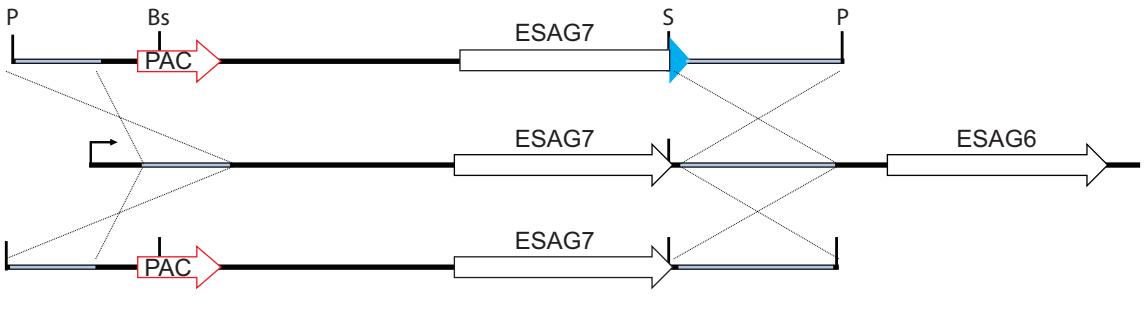

Changing BES7-VSG224 to BES7-VSG221

VSG224 genomic locus

replacement construct

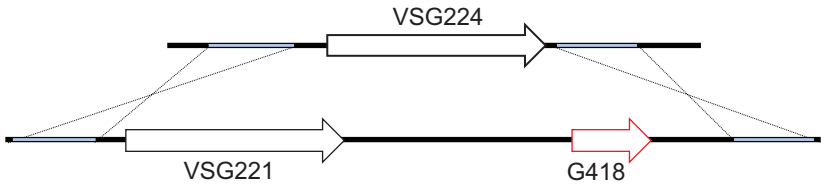

B

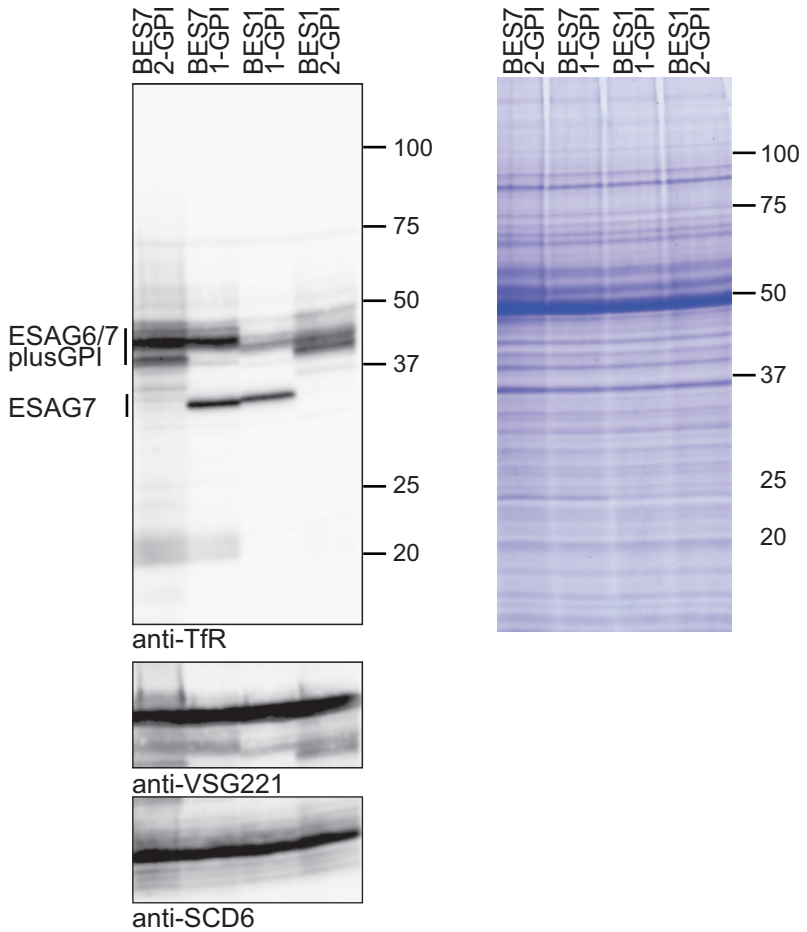

C

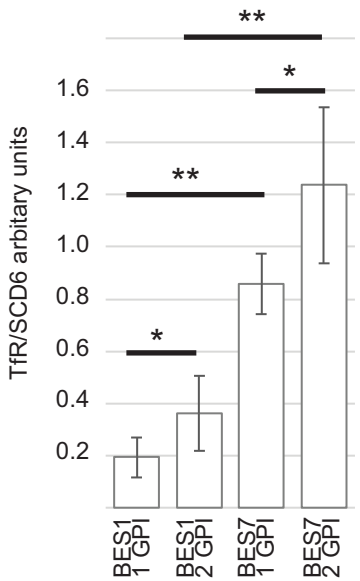

Figure 2

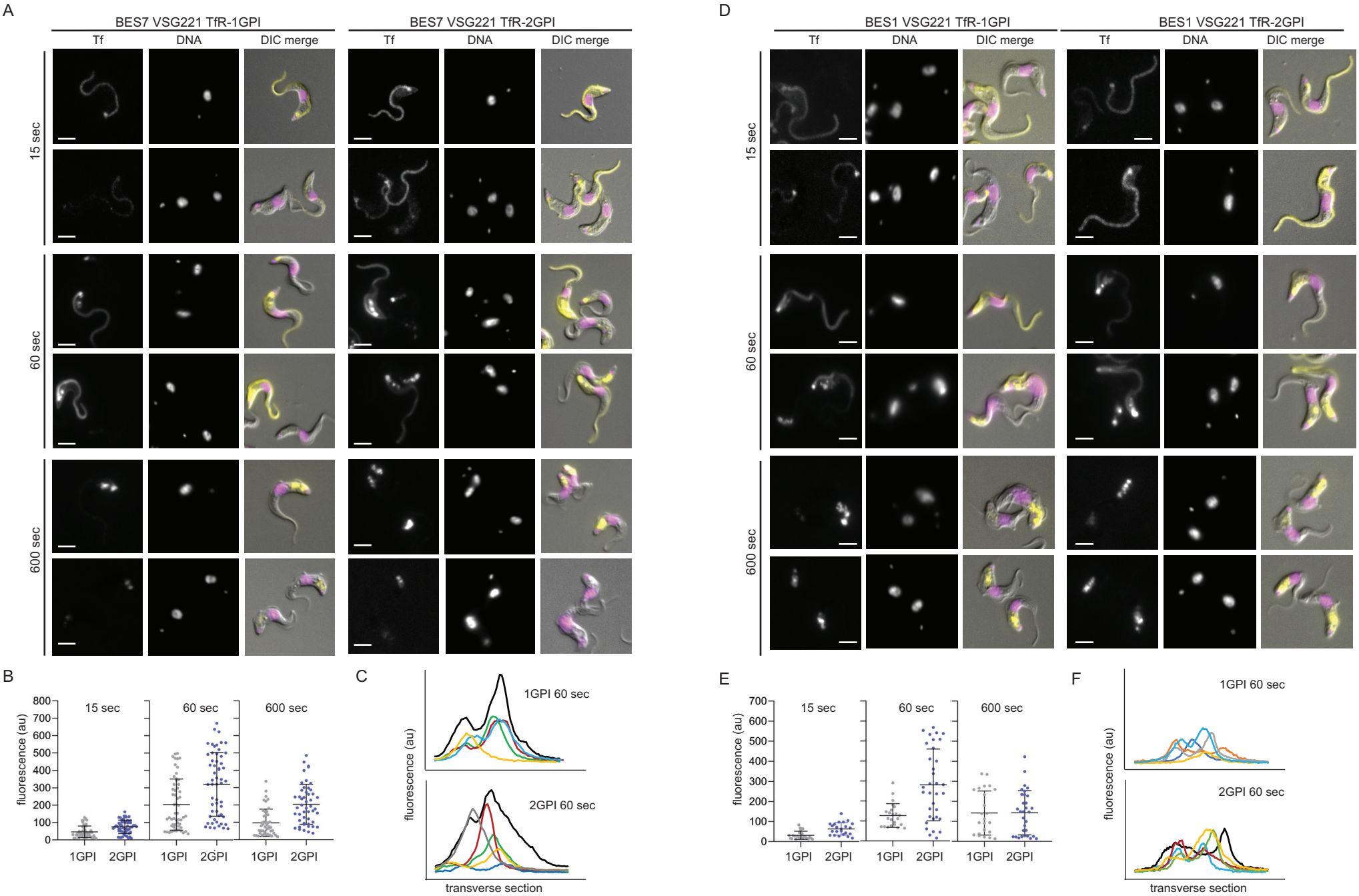
A
BES7 VSG221 TfR-1GPI
BES7 VSG221 TfR-2GPI
Tf
DNA
DIC merge
15 sec
60 sec
600 sec
D
BES1 VSG221 TfR-1GPI
BES1 VSG221 TfR-2GPI
B
fluorescence (au)
15 sec
60 sec
600 sec
1GPI
2GPI
C
1GPI 60 sec
2GPI 60 sec
transverse section
E
F

Figure 3

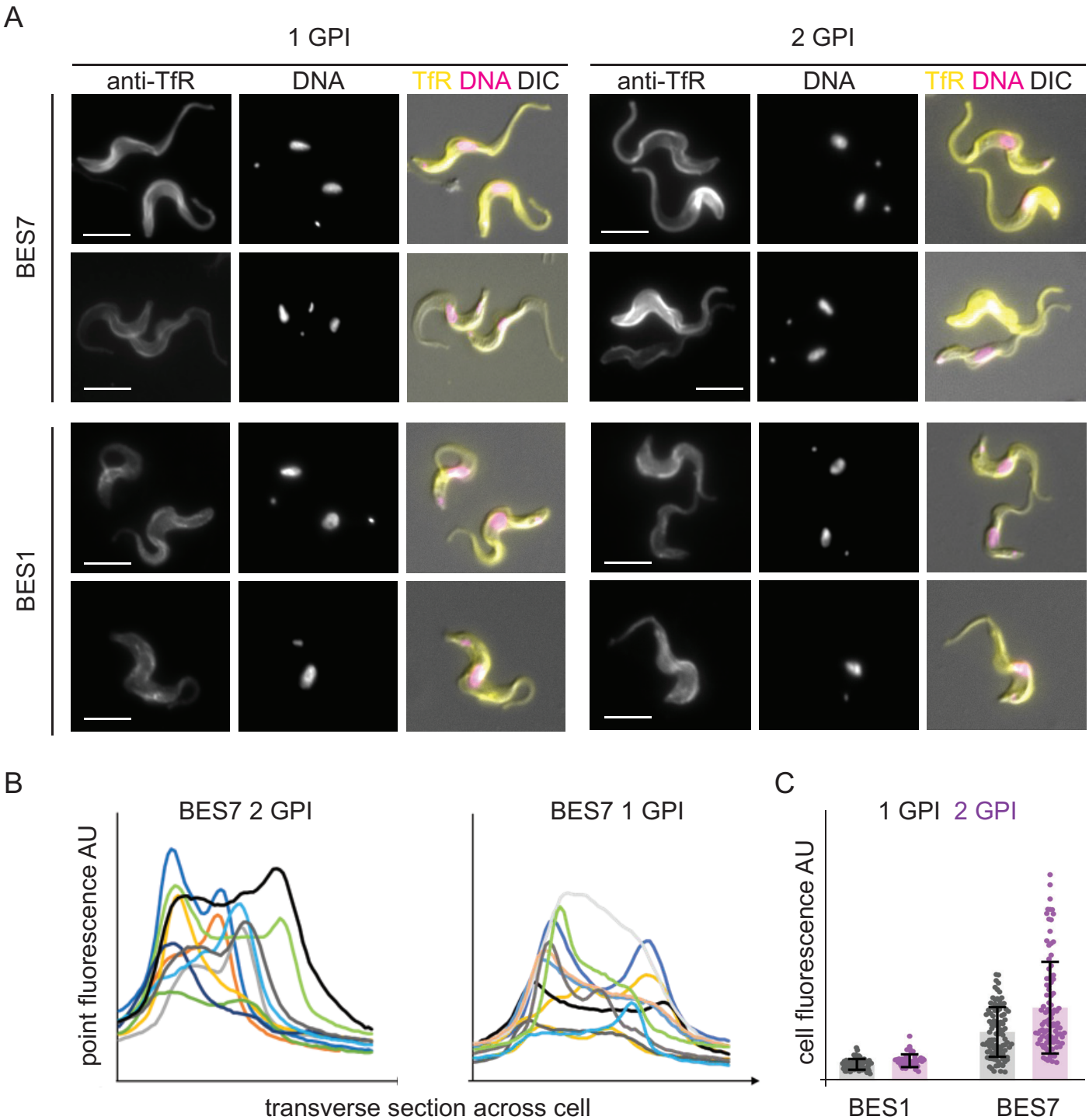
A
1 GPI
2 GPI
anti-TfR
DNA
TfR DNA DIC
anti-TfR
DNA
TfR DNA DIC
BES7
BES1
B
BES7 2 GPI
BES7 1 GPI
point fluorescence AU
transverse section across cell
C
1 GPI 2 GPI
cell fluorescence AU
BES1
BES7

Figure 4

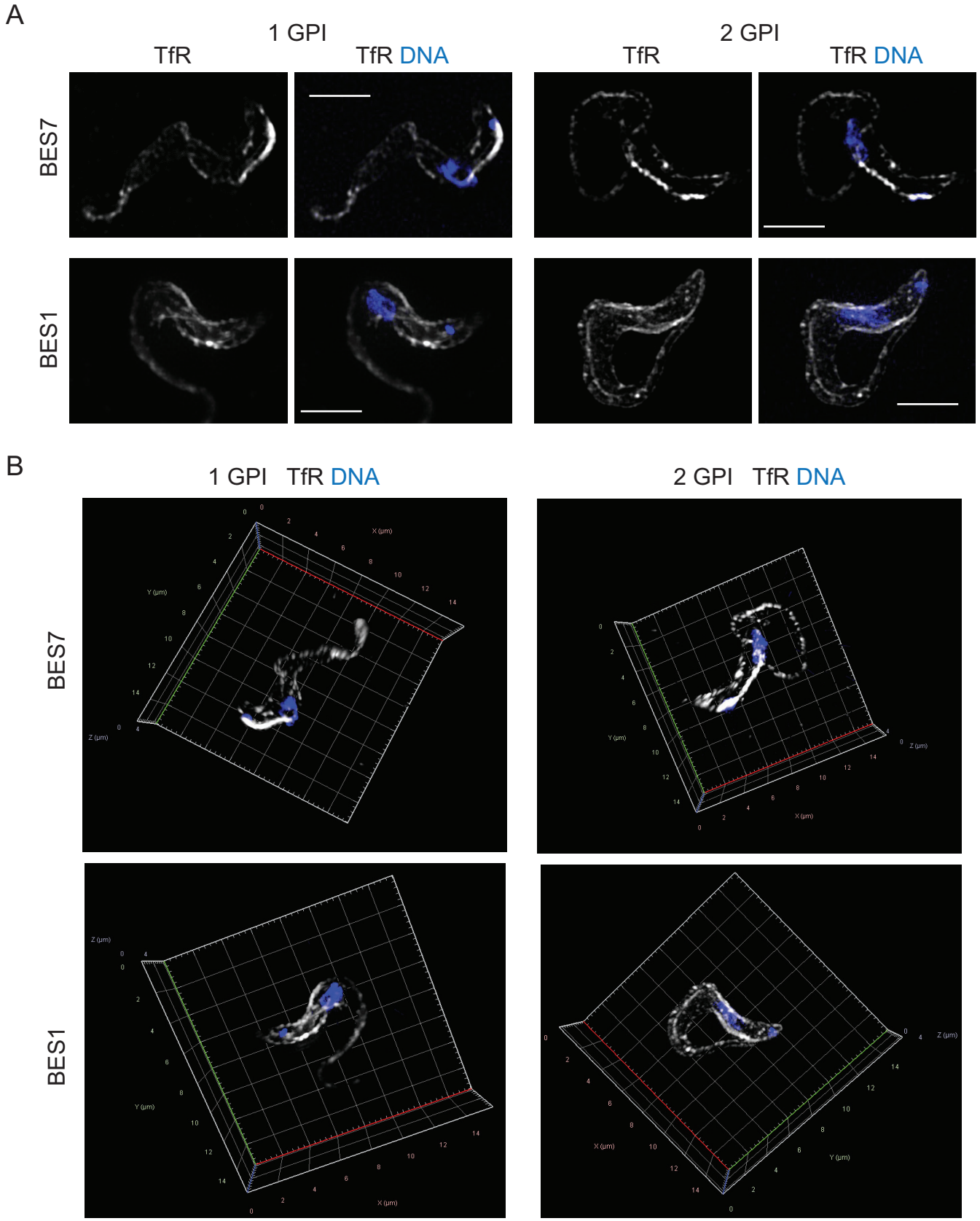
A
1 GPI
2 GPI
TfR
TfR DNA
TfR
TfR DNA
BES7
BES1
B
1 GPI TfR DNA
2 GPI TfR DNA
BES7
BES1

Figure 5

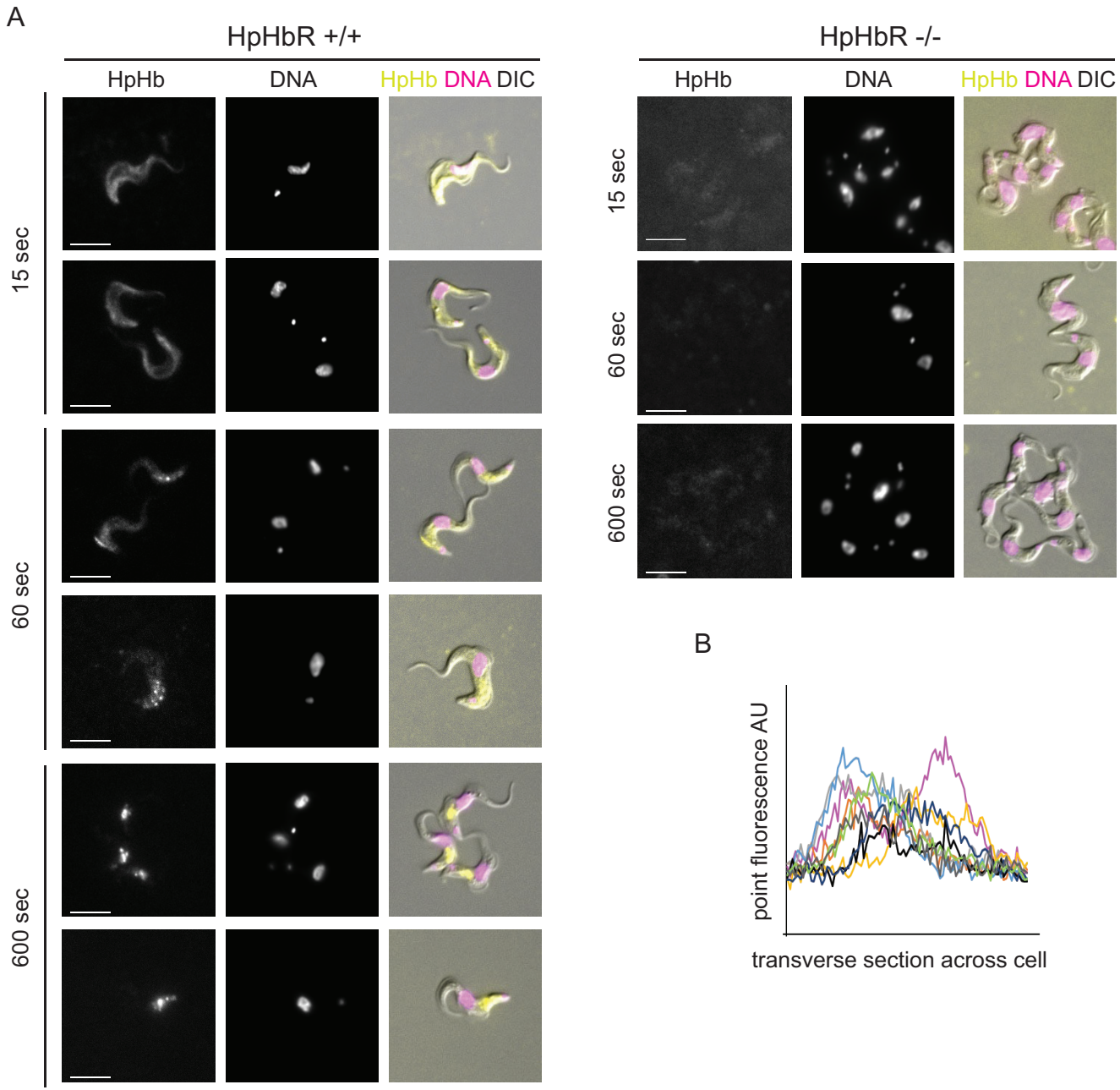
A
HpHbR +/+
HpHbR -/-
HpHb
DNA
HpHb DNA DIC
15 sec
60 sec
600 sec
B
point fluorescence AU
transverse section across cell

Figure 6

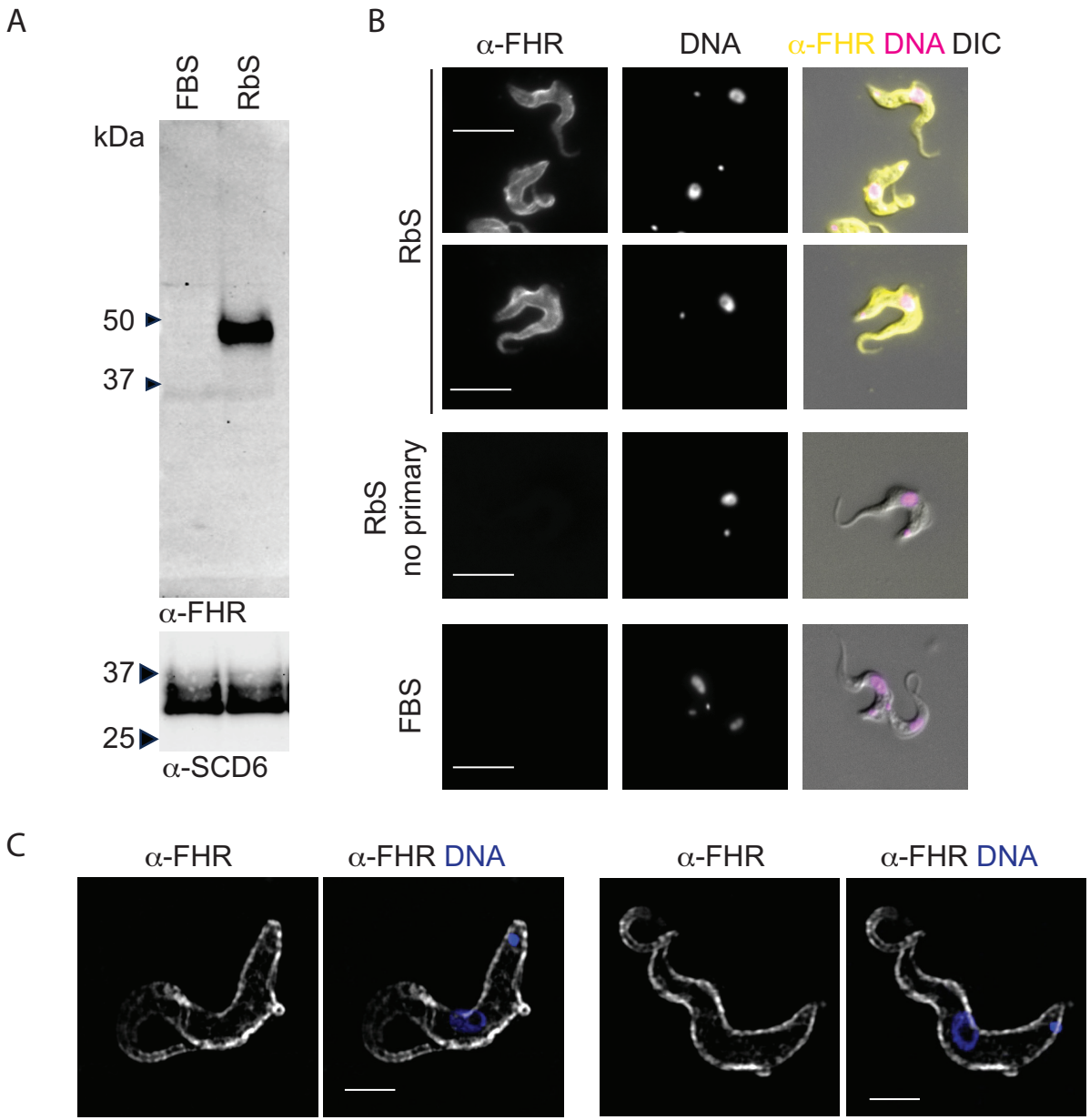
A
FBS
RbS
kDa
50
37
α-FHR
37
25
α-SCD6
B
α-FHR
DNA
α-FHR DNA DIC
RbS
RbS
no primary
FBS
C
α-FHR
α-FHR DNA
α-FHR
α-FHR DNA

Figure 7

A
ESAG7 ORFs from ~base 840

```
BES11    TTTAAGGATGTCATTCGCCTGTTTGCGCGCTTCAAAGAAGCAAAAAATGCAGTGATGAAGAAAATAAAAACTACTGTGGATGAATTGACTAAATGCATAGGGCAGAAAGAGGCTGAGCTC
BES2     TTTAAGGATGTCATCCGCCTGTTTGCGCGCTTCCAAGAAGCAAAAAATGCAGTGATGAATAAAATAAAAACTACTGTGGATGAATTGGCGAAATGCATAGGGCAGAAAGAGGTTGAGCTC
BES1     TTTAAGGATGTCATCCGCCTGTTTGCGCGCTTCCAAGAAGCAAAAAATGCAGTGATGAATAAAATAAAAACTACTGTGGATGAATTGGCGAAATGCATAGGGCAGAAAGAGGTTGAGCTC
BES4     TTTAAGGATGTCATTCGCCTGTTTGCGCGCTTCCAAGAAGCAAAAAATGCAGTGATGAATAAAATAAAAACTACTGTGGATGAATTGGCGAAATGCATAGGGCAGAAAGAGGTTGAGCTC
BES5     TTTAAGGATGTCATTCGCCTGTTTGCGCGCTTCCAAGAAGCAAAAAATGCAGTGATGAATAAAATAAAAACTACTGTGGATGAATTGGCGAAATGCATAGGGCAGAAAGAGGTTGAGCTC
BES7     TTTAAGGATGTCATTCGCCTGTTTGCGCGCTTCCAAGAAGCAAAAAATGCAGTGATGACGAAAATAAAAACTACTGTGGATGAATTGACGAAATGCATAGGGCAGAAGGAGGCTGAGCTC
BES13    TTTAAGGATGTCATTCGCCTGTTTGCGCGCTTCCAAGAAGCAAAAAATGCAGTGATGAGGAGAATAAAAACTACTGTGGATGAATTGACGAAATGTATAGGGAAGAAGGAGGCTGAACTC
BES14    TTTAAGGATGTCATTCGCCTGTTTGCGCGGTTCCAAGAAGCAAAAAATGAAGTGATGAATAAAATAAAAACTACTGTGGATGAATTGGCGAAATGCATAGGGCAGAAAGAGGTTGAGCTC
BES15    TTTAAGGATGTCATTCGCCTGTTTGCGCGGTTCCAAGAAGCAAAAAATGCAGTGATGACGAAAATAAAAACTACTGTGGATGAATTGACGAAATGCATAGGGCAGAAGGAGGCTGAACTC
BES12    TTTAAGGATGTCATTCGACTGTTTGCGCGCTTCCAAGAAGCAAAAAATGCAGTGATGAAGAAAATAAAAACTACTGTGGATGAATTGACGAAATGCATAGGGCAGAAAGAGGCTGAGCTC
BES3     TTTAAGGATGTCATTCGCCTGTTTGCGCGCTTCCAAGAAGTAAAAAATGCAGTGATGAAGAAAATAAAAACTACTGTGGATGAATTGACGAAATGCATAGGGCAGAAAGAGGCTGAGCTC
BES10    TTTAAGGATGTCATTCGCCTGTTTGCGCGCTTCCAAGAAGCAAAAAATGCAGTGATGAAGAAAATAAAAACTACTGTGGATGAATTGACGAAATGCATAGGGCAGAAGGAGGCTGAACTC
BES17    TTTAAGGATGTCATTCGCCTGTTTGCGCGCTTCCAAGAAGTAAAAAATGCAGTGGTGAAGAAAATAAAAACTACTGTGGATGAATTGACGAAATGCATAGGGCAGAAAGAGGCTGAGCTC
         ************** ** *********** *** ****** ******** **** ***  * ************************* * ***** ****** **** **** *** ***

BES11    ACTAATGATCAGCTTTACGAGGAATTT------GAGGCAATA----------------CAAAAGTATCTAGG-----------TTTTGGTAAAATGGAGTAAAAGC-----AAATTCAAC
BES2     ACTAATGATCAGCTTTACGAGGAATTC------GAGGCAATA----------------CAAAAGTACCTAGGG----------TCTCTGTGAAATGGAGTAAAAGC-----GAATTCAAC
BES1     ACTAATGATCAGCTTTACGAAGAATTC------GAGGCAATA----------------CAAAAGTACCTAGGG----------TCTCTGTGAAATGGAGTAAAGGC-----GAATTCAAC
BES4     ACTAATGATCAGCTTTACGAGGAATTC------GAGGCAATA----------------CAAAAGTACCTAGGG----------TCTCTGTGAAATGGAGTAAAAGC-----GAATTCAAC
BES5     ACTAATGATCAGCTTTACGAGGAATTC------GAGGCAATA----------------CAAAAGTACCTAGGG----------TCTCTGTGAAATGGAGTAAAAGC-----TAATTCAAC
BES7     ACTAATGATCAGCTTTACGAGGAATTTTATCTGGGAGACCATAAACAGATTGGAGCTGTCAAAGAGAGTGAGTGAACAACCCTCTTTAGGTGAAGAAGAGGAGACGATCCTGAAATCTAAC
BES13    ACTAATGATCAGATTTACGAGGAATTC------GAGGCAATA----------------CAAAAGTATCTAGGG----------TTTCTGTGAAATGGAGTAAAAGC-----GAATCTAAC
BES14    ACTGATGATCAGCTTTACGAGGAATTC------GAGGCAATA----------------CAAAAGTATCTAGGG----------TTTCTGTGAAATGAAGTAAAAGC-----GAATCTAAC
BES15    ACTAATGATCAGATTTACGAGGAATTC------GAGGCAATA----------------CAAAAGTATCTAGGG----------TTTCTGTGAAATGGAGTAAAAGC-----GAATTTAAC
BES12    ACTAATGATCAGCTTTACGAGGAATTT------GAGGCAATA----------------CAAAAGTATCTAGGG----------TTTCTGTGAAATGGAGTAAAAGC-----GAATTTAAC
BES3     ACTAATGATCAGCTTTACGAGGAATTT------GAGGCAATA----------------CAAAAGTATCTATGG----------TTTCTGTGAAATGGAGTAAAAAC-----GAATCTAAC
BES10    ACTAATGATCAGATTTACGAGGAATTC------GAGGCAATA----------------CAAAAGTATCTAGGG----------TTTCTGTGAAATGGAGTAAAATC-----GAATCTAAC
BES17    ACTAATGATCAGCTTTACGAGGAATTT------GAGGTAATA----------------CAAAAGTATCTATGG----------TTTCTGTGAAATGGAGTAAAAAC-----GAATCTAAC
         *** ******** ******* *****       ***   ***                 ****   *   *             * *  ** **    ** * *         ***  ***

BES11    TATACTGTAGAGCCTGTCTGGGGACCTTTCACGGGAGCGGGGTCCAACGCGGCAGCAATACATTCGAGTGTATCTACCGCTGCACTCTGTTGTTCAGTTTTATTGTTTGGAGTGCTGTGA
BES2     TATACTGCAGAACCGGTCCGGGGACATTTCACGGGAGCGGGGTCCAACGCGGCAGCAGTACATTTGAGTGTTTCTACCGCTGCACTTTGTTTTTCAGTTTTATTGTTGGGAGTGCTGTGA
BES1     TATACTGCAGAACCGGTCCGTGGACCTTTCACGGTAGCGGGGTCCAACACAGTAGCAGTACATTTGAGTGTTTCTACCGCTGCACTTTGTTTTTCAGTTTTATTGTTGGGAGTGCTGTGA
BES4     TATACTGCAGAACCGGTCCGGGGACATTTCACGGGAGCGGGGTCCAACGCGGCAGCAGTACATTTGAGTGTTTCTACCGCTGCACTTTGTTTTTCAGCTTTATTGTTGGGAGTGCTGTGA
BES5     TATACTGCAGAACCGGTCCGGGGACATTTCACGGGAGCGGGGTCCAACGCGGCAGCAGTACATTTGAGTGTTTCTACCGCTGCACTTTGTTTTTCAGCTTTATTGTTGGGAGTGCTGTGA
BES7     TATACTGCAGAACCTGTCCGTGGACCTTTCACGGGAGCGGGGGCCAACACAGTAGCAGTACAGTCGAGTGTTTCTACCGCTGCACTTTGTTGTTCAGCTTTATTGTTGGGAGTGCTGTGA
BES13    TATACTGTAGAACCTGTCCGTGGACCTTTCACGGGAGCGGGGTCCAACACAGTAGCAGTACATTTGAGTGTTTCTACCGCTGCACTCTGTTGTTTAGCTTTATTGTTGGGAGTGCTGTGA
BES14    TATACTGCAGAACCTGTCCGTGGACCTTTCACGGGAGCGGGGTCCAACACAGTAGCAGTACATTTGAGTGTTTCTACCGCTGCACTTTGTCGTTCAGCTTTATTGTTGGGAGTGCTGTGA
BES15    TATACTGCAGAACCTGTCCGTGGACCTTTCACGGGAGCGGGGTCCAACACAGTAGCAGTACAGTCGAGTGTTTCTACCGCTGCACTTTGTTGTTCAGTTTTATTGTTGGGAGTGCTGTGA
BES12    TATACTGCAGAACCTGTCCGTGGACCTTTCACTGGAGCGGGGGCCAATGCGGCAGCAATACATTTGAGTGTTTCTACCGCTGCACTTTGTTGTTCAGCTTTATTGTTGGGAGTGCTGTGA
BES3     TATACTGCAGAGCCTGTCCGTGGACCTTTAACGGGAGCGGGGGCCAACGCGGCAGCAATACATTTGAGTGTTTCTACCGCTGCACTTTGTCGTTCAGCTTTATTGTTGGGAGTGCTGTGA
BES10    TATACTGCAGAGCCTGTCCGTGGACCTTTAACGGGAGCGGGGGCCAACGCGGCAGCAATACATTTGAGTGTTTCTACCGCTGCACTTTGTCGTTCAGCTTTATTGTTGGGAGTGCTGTGA
BES17    TATACTGCAGAGCCTGTCCGTGGACCTTTCACGGTAGCGGGGGCCAACGCGGCAGCAATACATTTGAGTGTTTCTACCGCTGCACTTTGTCGTTCAGCTTTATTGTTGGGAGTGCTGTGA
         ******* *** ** *** * **** *** ** * ******* ****  * * **** **** * ****** ************** ***  ** ** ********* ******** ***
```

B

Comparison of ESAG7 from BES1 and BES7

```
         F  K  D  V  I  R  L  F  A  R  F  Q  E  A  K  N  A  V  M  T  K  I  K  T  T  V  D  E  L  T  K  C  I  G  Q  K  E  A  E  L
BES7     TTTAAGGATGTCATTCGCCTGTTTGCGCGCTTCCAAGAAGCAAAAAATGCAGTGATGACGAAAATAAAAACTACTGTGGATGAATTGACGAAATGCATAGGGCAGAAGGAGGCTGAGCTC
BES1     TTTAAGGATGTCATCCGCCTGTTTGCGCGCTTCCAAGAAGCAAAAAATGCAGTGATGAATAAAATAAAAACTACTGTGGATGAATTGGCGAAATGCATAGGGCAGAAAGAGGTTGAGCTC
F1        F  K  D  V  I  R  L  F  A  R  F  Q  E  A  K  N  A  V  M  N  K  I  K  T  T  V  D  E  L  A  K  C  I  G  Q  K  E  V  E  L

         T  N  D  Q  L  Y  E  E  F  I  W  E  T  I  N  R  L  E  L  S  K  R  V  S  E  Q  P  S  L  G  E  E  E  E  T  I  L  K  S  N
BES7     ACTAATGATCAGCTTTACGAGGAATTTATCTGGGAGACCATAAACAGATTGGAGCTGTCAAAGAGAGTGAGTGAACAACCCTCTTTAGGTGAAGAAGAGGAGACGATCCTGAAATCTAAC
BES1     ACTAATGATCAGCTTTACGAAGAATTC------GAGGCAATA----------------CAAAAGTACCTAGGG--------TCTCTGTGAAATGGAGTAAAGGC------GAATTC-AAC
F1        T  N  D  Q  L  Y  E  E  F       E  A  I                Q  K  Y  L  G         S  L  *                          N

         Y  T  A  E  P  V  R  G  P  F  T  G  A  G  A  N  T  V  A  V  Q  S  S  V  S  T  A  A  L  C  C  S  A  L  L  L  G  V  L  *
BES7     TATACTGCAGAACCTGTCCGTGGACCTTTCACGGGAGCGGGGGCCAACACAGTAGCAGTACAGTCGAGTGTTTCTACCGCTGCACTTTGTTGTTCAGCTTTATTGTTGGGAGTGCTGTGA
BES1     TATACTGCAGAACCGGTCCGTGGACCTTTCACGGTAGCGGGGTCCAACACAGTAGCAGTACATTTGAGTGTTTCTACCGCTGCACTTTGTTTTTCAGTTTTATTGTTGGGAGTGCTGTGA
F1        Y  T  A  E  P  V  R  G  P  F  T  V  A  G  S  N  T  V  A  V  H  L  S  V  S  T  A  A  L  C  F  S  V  L  L  L  G  V  L  *
```

Supp Figure 1

```
BES7-6       MMRFWFVLLALLGKETY--AYENERNALNATAANKVCGLSTYLKGIAHRVNSESAVVTEK     58
BES7-7       -MRFLFVLLALLGKETHANYYENERNALNATAANKVCALSTYLKGIAHRVNSESAVVTEK     59
              *** ***********:   *****************.**********************

BES7-6       LSDLKMRSIQLQLSVMRNRVPSGEKDCKDIRTLLKTVLRNEFTFQQELEEMRSASALAAA     118
BES7-7       LSDLKMRSIQLQLSIMRNRVPSGEKDCKDIRTLLKTVLRNEFTFQQELEEVRNASALAAA     119
             **************:***********************************:*.*******

BES7-6       AAGLAAGRLEEWIFVFAQAADGSSQFCISVGKTIPAEHGDLQECFDGKIGPETLYKIEDS     178
BES7-7       AAGLAAGRLEEWIFVFAQAGGRSSQFCISTGKTGPAEYNNLQECFDGTIGPETLYKIEDS     179
             *******************.. *******.*** ***:.:*******.************

BES7-6.      RVKESAQKSLQLHEVLSSISFGSLGVKNIVEKGENRGCNLMRTADEGLLKDVC-LNRNFT     237
BES7-7       RVKESAKTRLLLHEVLSSISFSSLGAENIRGGNGKDGCNLVRTDNNGILKGGSPTRHNLT     239
             ******:. * **********.***.:**   . : ****:** ::*:**. .  .:*:*

BES7-6       WGGGVLNFGYCVAGNLKIKGGEYGDVSSYDAVRWTEDPSKVSIFKDVIRLFARFQEAKNA     297
BES7-7       WGGGVMNFGSYQNGSMYVEGGEYGDATEYGAVRWTEDPSKVSIFKDVIRLFARFQEAKNA     299
             *****:***    *.: ::******.:.*.******************************

BES7-6       VMTKIKTTVDELTKCIGQKEAELTNDQLYEEFIWETINRLELSKRVSEQPSLGEEEETIL     357
BES7-7       VMTKIKTTVDELTKCIGQKEAELTNDQLYEEFIWETINRLELSKRVSEQPSLGEEEETIL     359
             ************************************************************

BES7-6       KSNYTAEPVRGPFTGAGANTVAVQSSVSTAALCCSALLLGVL     399
BES7-7       KSNYTAEPVRGPFTGAGANTVAVQSSVSTAALCCSALLLGVL     401
             ******************************************
```

```
# NetGPI 1.1      Timestamp: 20240925160446
# ID  Seq-length  Pred. GPI-Anchored      Omega-site pos.   Likelihood  Amino-acid
Sequence    399        GPI-Anchored      372                  0.438          G
```

ESAG6

```
# SignalP-6.0     Organism: Eukarya Timestamp: 20250215202022
# ID  Prediction  OTHER SP(Sec/SPI) CS Position
Sequence    SP    0.000369    0.999614    CS pos: 17-18. Pr: 0.9774
```

ESAG7

```
# SignalP-6.0     Organism: Eukarya Timestamp: 20250215202326
# ID  Prediction  OTHER SP(Sec/SPI) CS Position
Sequence    SP    0.000332    0.999656    CS pos: 18-19. Pr: 0.9760
```

Supp Figure 2

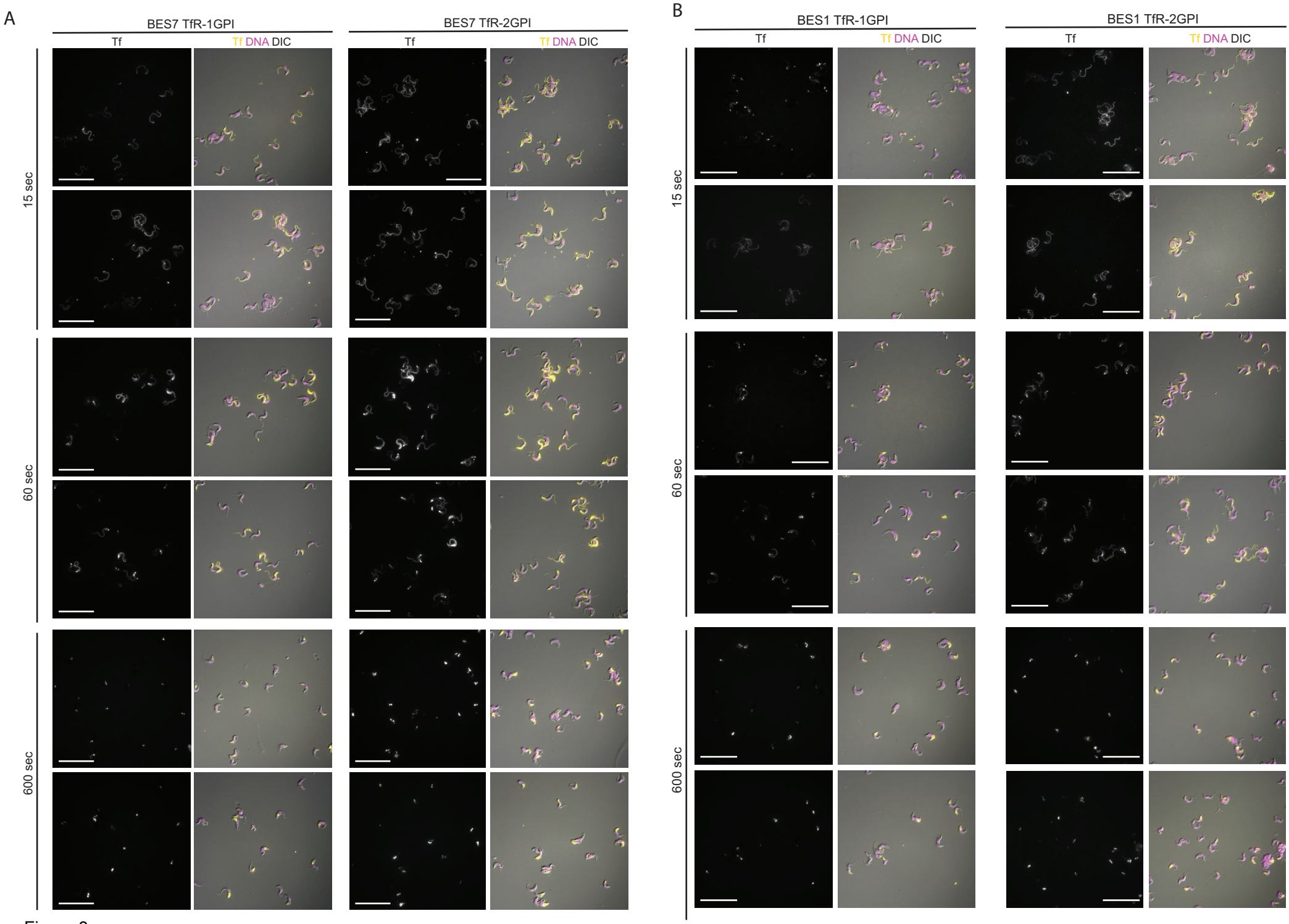

Supp Figure 3

A

```
cow      -DPERTVRWCTISTHEANKCASFRENVLRILESGPFVSCVKKTSHMDCIKAISNNEADAV     59
dog      VSPEKTVRWCTVSNHEASKCSSFMENMKTVLENGPFVSCVKRTSYLECIKAIWANEADAV     60
          .**:******:*.***.**:** **:  :**.********:**:::*****  ******

cow      TLDGGLVYEAGLKPNNLKPVVAEFHGTKDNPQTHYYAVAVVKKDTDFKLNELRGKKSCHT     119
dog      TLDAGLVFEAGLNPYNLKPVVAEFYGKD--KQTRYYAVAVVKKSSTFNLNQLQGKKSCHT     118
         ***.***:****:* *********:*..   **:*********.: *:**:*:*******

cow      GLGRSAGWNIPMGKLYKELPDPQESIQRAAANFFSASCVPCADQSSFPKLCQLCAGKGTD     179
dog      GLGRSAGWNIPMGLLYWKLPEPRESLQKAASSFFTASCVPCVDRTAFPKLCQLCVGKGTD     178
         ************* ** :**:*:**:*:**:.**:******.*:::********.*****

cow      KCACSNHEPYFGYSGAFKCLMEGAGDVAFVKHSTVFDNLPNPEDRKNYELLCGDNTRKSV     239
dog      KCACSNHEPYFGYSGAFKCLMEDAGEVAFVKHSTVLENLPNKADLDQYELLCPDNKRKPV     238
         **********************.**:*********::****  * .:***** **.** *

cow      DNYQECYLAMVPSHAVVARTVGGKEDVIWELLNHAQEHFGKDKPDNFQLFQSPHGKDLLF     299
dog      GEYKQCYLAKVPSHAVVARSVGGKEDLIWELLNQAQEHYGKDKSKVFQLFSSTLGKDLLF     298
         .:*::**** *********:******:******:****:**** . ****.*  ******

cow      KDSADGFLKIPSKMDFELYLGYEYVTALQNLRESKPPDSSKDECM-VKWCAIGHQERTKC     358
dog      KDSAEGFFRIPPKMDTWLYLGYEYVTALRNLREDVRPDTPRDECKKVKWCAVGHHEIAKC     358
         ****:**::** ***  ***********:****.  **: :***  *****:**:* :**

cow      DRWSGFSGGAIECETAENTEECIAKIMKGEADAMSLDGGYLYIAGKCGLVPVLAENYKTE     418
dog      DEWSVNSEGKIECESAESTEDCIAKIAKGEADAMSLDGGYIYIAGQCGLVPVLAENYKTQ     418
         *.**  * * ****:**.**:***** *************:****:*************:

cow      DGSCKNTPEKGYLAVAVVKTSDANINWNNLKGKKSCHTAVDRTAGWNIPMGLLYSKINNC     478
dog      GSTCSNTAEEGYLAVAVVKELDKTISWNNLQGRKSCHTAVDRTAGWNIPMGLLYNRINHC     478
         ..:*.** *:*********  * .*.****:*:**********************.:**:*

cow      KFDEFFSAGCAPGSPRNSSLCALCIGSEKGTGKECVPNSNERYYGYTGAFRCLVEKGDVA     538
dog      EFDKFFSQGCAPGSMRNSSLCALCIGSANVPGKECVPNNHERYYGYTGAFRCLVEKGDVA     538
         :**:*** ****** ************ :  *******.:********************

cow      FVKDQTVIQNTDGNNNEAWAKNLKKENFEVLCKDGTRKPVTDAENCHLARGPNHAVVSRK     598
dog      FVKDQTVLQNTGGKNTEDWAKDLKEEDFELLCPDGQRKSVDKAPECFLAKAPNHAVVSRK     598
         *******:***.*:*.* ***:**:*:**:** ** ** * .* :*.**:.*********

cow      DKATCVEKILNKQQDDFGKSVTDCTSNFCLFQSNSKDLLFRDDTKCLASIAK-KTYDSYL     657
dog      DKASCVSKMLLDQQLLFGRNGNDCSGKFCLFHSATKDLLFRDDTQCLAKLPEDTTYKSYL     658
         ***:**.*:* .**  **:. .**:.:****:* :*********:***.: : .**.***

cow      GDDYVRAMTNLRQCSTSKLLEACTFHKP   685
dog      GAEYITAVANLRQCSTSKLLEACTFHTS   686
         * :*: *::*****************.

Identities
501/686
```

B

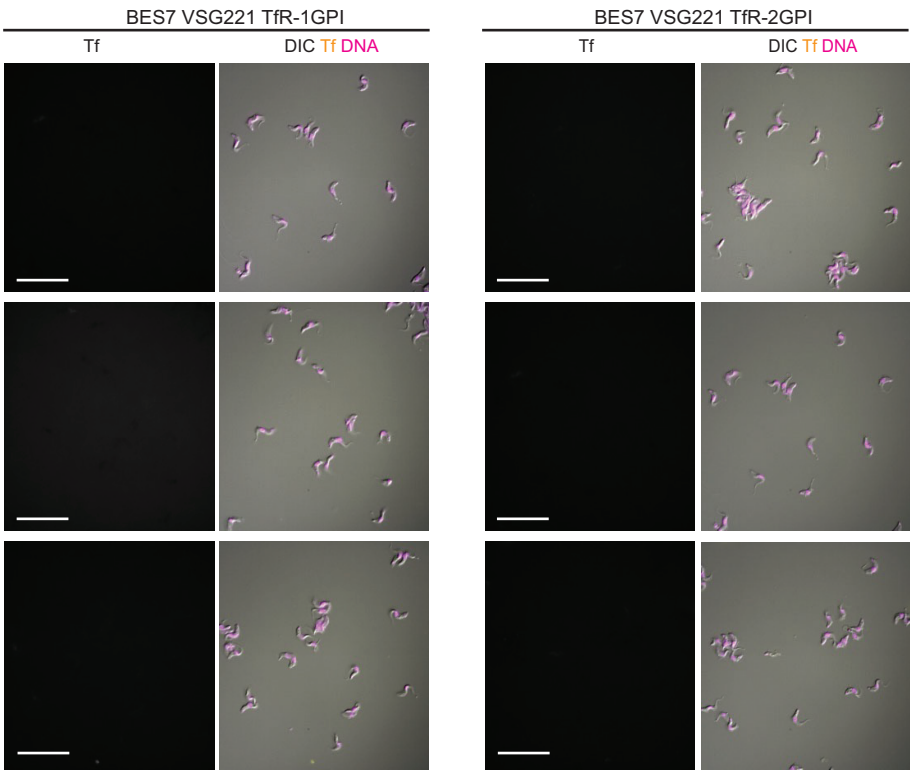

Supp Figure 4

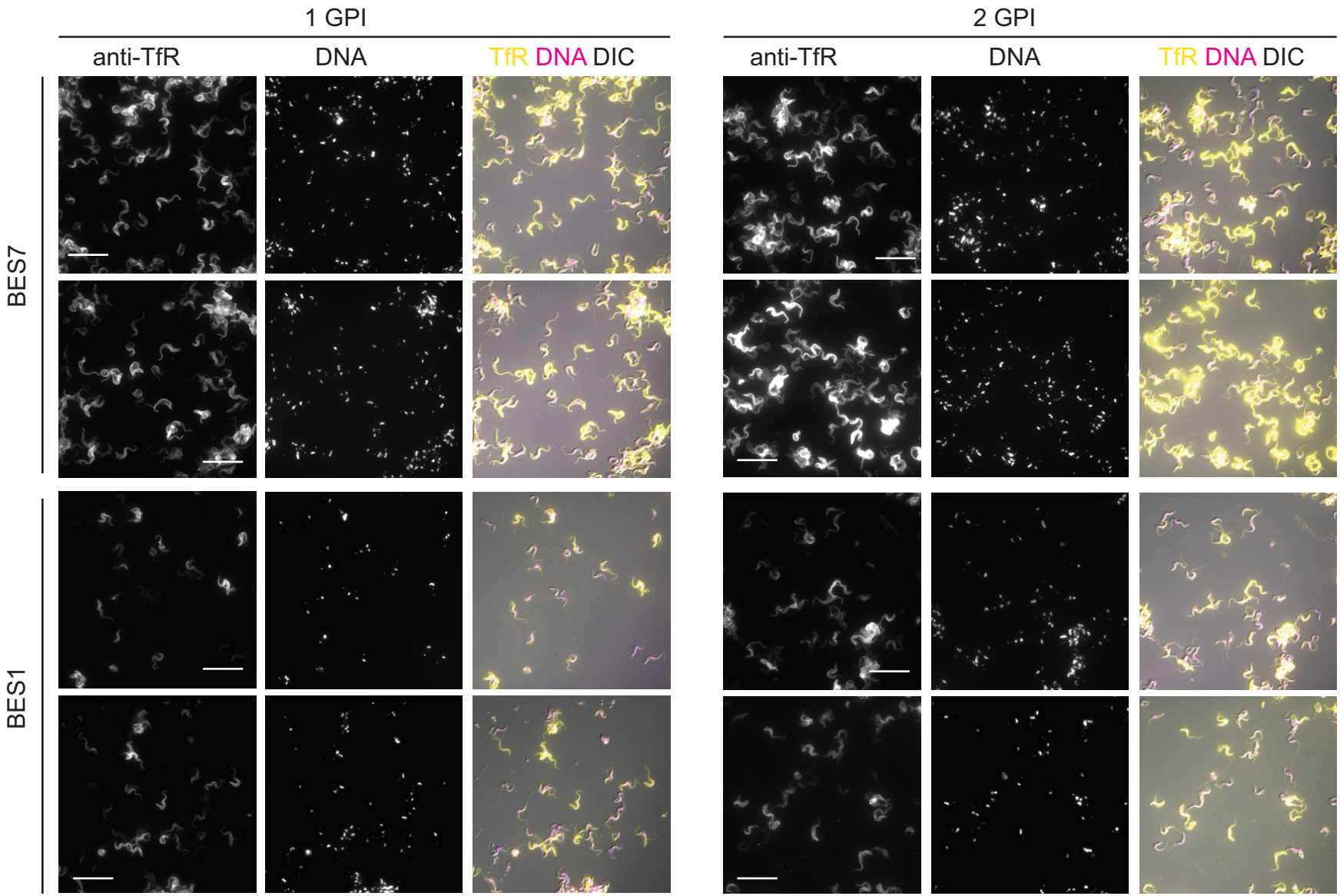

Supp Figure 5

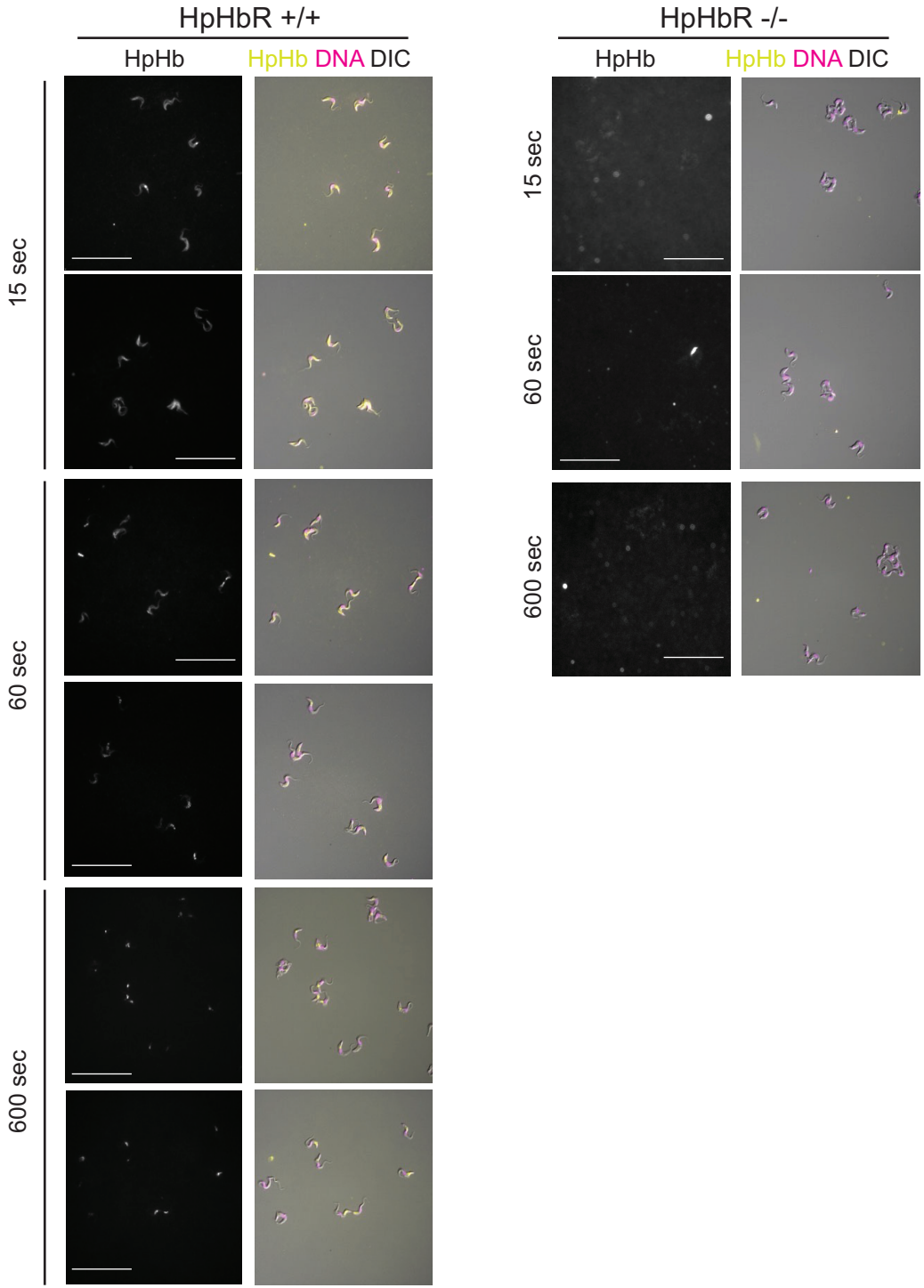

Supp Figure 6

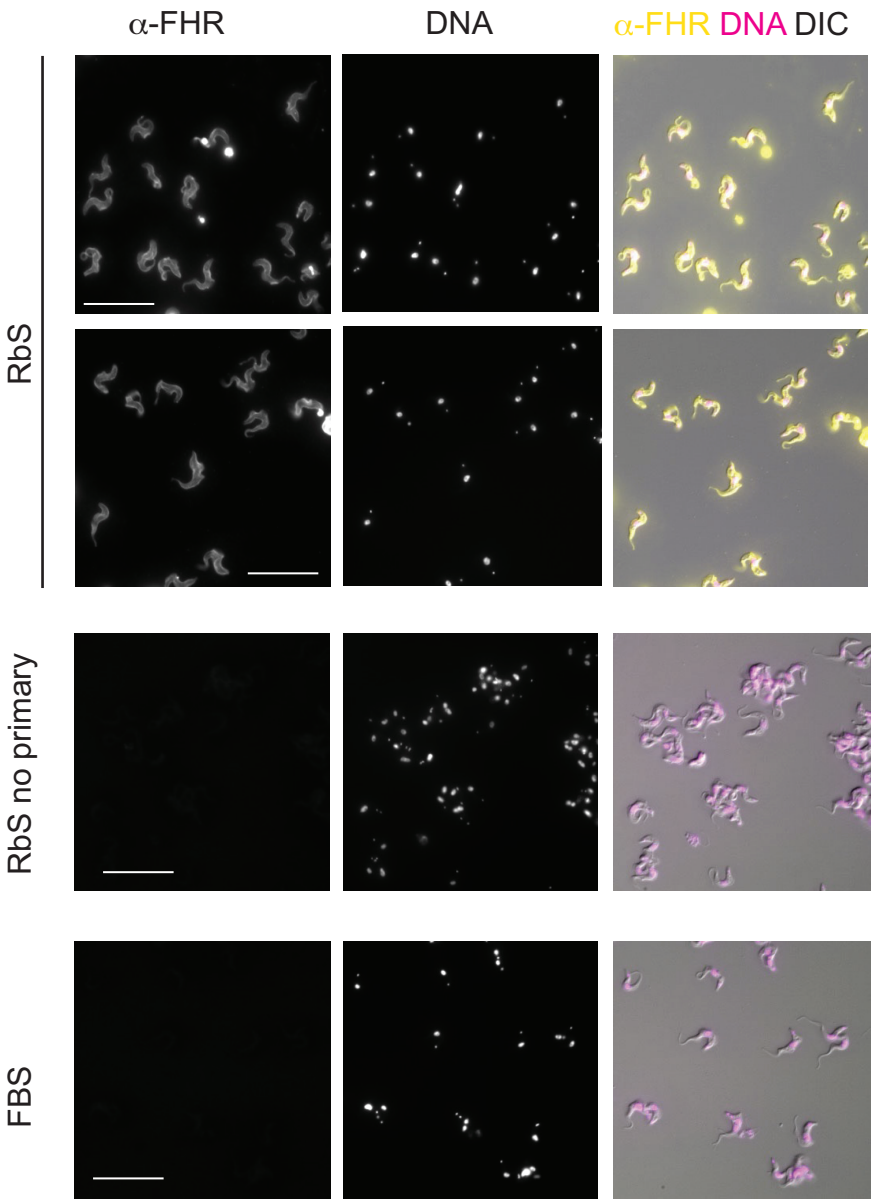

Supp Figure 7